IJMMM International Journal of Minerals, Metallurgy and Materials 矿物冶金与材料学报（英文版）

Review of recent advances in ferrite-based materials: From synthesis techniques to electromagnetic wave absorption performance

Xingliang Chen, Di Lan, Luoting Zhou, Hailing Liu, Xiyu Song, Shouyu Wang, Zhuanyong Zou, and Guanglei Wu

Cite this article as:
Xingliang Chen, Di Lan, Luoting Zhou, Hailing Liu, Xiyu Song, Shouyu Wang, Zhuanyong Zou, and Guanglei Wu, Review of recent advances in ferrite-based materials: From synthesis techniques to electromagnetic wave absorption performance, *Int. J. Miner. Metall. Mater.*, 32(2025), No. 3, pp. 591-608. https://doi.org/10.1007/s12613-024-3063-9

View the article online at SpringerLink or IJMMM Webpage.

Articles you may be interested in

Zhenguo Gao, Kai Yang, Zehao Zhao, Di Lan, Qian Zhou, Jiaoqiang Zhang, and Hongjing Wu, Design principles in MOF-derived electromagnetic wave absorption materials: Review and perspective, *Int. J. Miner. Metall. Mater.*, 30(2023), No. 3, pp. 405-427. https://doi.org/10.1007/s12613-022-2555-8

Shijie Zhang, Jiying Li, Xiaotian Jin, and Guanglei Wu, Current advances of transition metal dichalcogenides in electromagnetic wave absorption: A brief review, *Int. J. Miner. Metall. Mater.*, 30(2023), No. 3, pp. 428-445. https://doi.org/10.1007/s12613-022-2546-9

Qiuyi Wang, Jie Liu, Yadong Li, Zhichao Lou, and Yanjun Li, A literature review of MOF derivatives of electromagnetic wave absorbers mainly based on pyrolysis, *Int. J. Miner. Metall. Mater.*, 30(2023), No. 3, pp. 446-473. https://doi.org/10.1007/s12613-022-2562-9

Bin Shi, Hongsheng Liang, Zijun Xie, Qing Chang, and Hongjing Wu, Dielectric loss enhancement induced by the microstructure of $CoFe_2O_4$ foam to realize broadband electromagnetic wave absorption, *Int. J. Miner. Metall. Mater.*, 30(2023), No. 7, pp. 1388-1397. https://doi.org/10.1007/s12613-023-2599-4

Xuanqi Yang, Honghan Wang, Jing Chen, Qingda An, Zuoyi Xiao, Jingai Hao, Shangru Zhai, and Junye Sheng, Customization of FeNi alloy nanosheet arrays inserted with biomass-derived carbon templates for boosted electromagnetic wave absorption, *Int. J. Miner. Metall. Mater.*, 31(2024), No. 4, pp. 812-824. https://doi.org/10.1007/s12613-023-2768-5

Jianghao Wen, Di Lan, Yiqun Wang, Lianggui Ren, Ailing Feng, Zirui Jia, and Guanglei Wu, Absorption properties and mechanism of lightweight and broadband electromagnetic wave-absorbing porous carbon by the swelling treatment, *Int. J. Miner. Metall. Mater.*, 31(2024), No. 7, pp. 1701-1712. https://doi.org/10.1007/s12613-024-2881-0

IJMMM WeChat

QQ author group

INTERNATIONAL JOURNAL OF
Minerals, Metallurgy and Materials

Volume 32, Number 3, March 2025
Page 591

Review https://doi.org/10.1007/s12613-024-3063-9

Review of recent advances in ferrite-based materials: From synthesis techniques to electromagnetic wave absorption performance

Xingliang Chen[1)], *Di Lan*[2)], *Luoting Zhou*[1)], *Hailing Liu*[1)], *Xiyu Song*[1)], *Shouyu Wang*[3)], *Zhuanyong Zou*[1),✉], *and Guanglei Wu*[4),✉]

1) Shaoxing Key Laboratory of High Performance Fibers & Products, Key Laboratory of Clean Dyeing and Finishing Technology of Zhejiang Province, Shaoxing University, Shaoxing 312000, China
2) School of Materials Science and Engineering, Hubei University of Automotive Technology, Shiyan 442002, China
3) Chinatesta (Zhejiang) Testing Services Co., Ltd., Shaoxing 312000, China
4) Institute of Materials for Energy and Environment, State Key Laboratory of Bio-fibers and Eco-textiles, College of Materials Science and Engineering, Qingdao University, Qingdao 266071, China
(Received: 12 June 2024; revised: 3 December 2024; accepted: 9 December 2024)

Abstract: With the booming development of electronic information science and 5G communication technology, electromagnetic radiation pollution poses a huge threat and damage to humanity. Developing novel and high-performance electromagnetic wave (EMW) absorbers is an effective method to solve the above issue and has attracted the attention of many researchers. As a typical magnetic material, ferrite plays an important role in the design of high-performance EMW absorbers, and related research focuses on diversified synthesis methods, strong absorption performance, and refined microstructure development. Herein, we focus on the synthesis of ferrites and their composites and introduce recent advances in the high-temperature solid-phase method, sol–gel method, chemical coprecipitation method, and solvent thermal method in the preparation of high-performance EMW absorbers. This review aims to help researchers understand the advantages and disadvantages of ferrite-based EMW absorbers fabricated through these methods. It also provides important guidance and reference for researchers to design high-performance EMW absorption materials based on ferrite.

Keywords: ferrite; electromagnetic wave absorber; sol–gel method; magnetic material; solvent thermal method

1. Introduction

1.1. EMW absorbing material

With the arrival of the fourth industrial revolution, human society has rapidly developed toward informatization and intelligence. Smartphones and 5G communication technology have become popular and made our daily lives convenient and efficient. However, the accompanying electromagnetic radiation pollution has also caused enormous harm to social development [1–5]. Long-term exposure to electromagnetic radiation may cause significant harm to human health, potentially leading to mental disorders and accelerating aging. Electromagnetic radiation pollution can also affect the operation of electronic instruments and medical equipment, leading to serious losses in social production and scientific research. Developing high-performance electromagnetic wave (EMW) absorbing materials is an effective strategy to solve the above issues and has attracted the attention of researchers worldwide [6–10].

EMW-absorbing materials can convert electromagnetic energy into other forms, such as thermal energy, and then dissipate it in the air to absorb or attenuate EMWs. For this goal, an ideal EMW-absorbing material should meet two necessary conditions, i.e., impedance matching characteristic and attenuation characteristic. When the EMW is incident on the absorber surface, the natural interface between the material and air has a reflection coefficient (R). R should be as small as possible so that much of the EMW incident on the material surface can enter the interior and the formation of external reflection can be avoided, thereby leading to improved EMW absorption efficiency. The magnitude of EMW's impedance (Z_{in}) and air impedance (Z_0) at the interface can directly determine the reflection coefficient R, and the relationship is shown as Eq. (1) [11–13]:

$$R = \frac{Z_{in} - Z_0}{Z_{in} + Z_0} \tag{1}$$

When the EMW is vertically incident on the surface of the absorbing material, Z_0 and Z_{in} can be expressed as Eqs. (2) and (3), respectively:

$$Z_0 = (\mu_0/\varepsilon_0)^{1/2} \tag{2}$$

$$Z_{in} = Z_0\left(\sqrt{\mu_r/\varepsilon_r}\right)\tanh\left[\mathrm{j}\left(\frac{2\pi f d}{c}\right)\left(\sqrt{\mu_r\varepsilon_r}\right)\right] \tag{3}$$

✉ Corresponding authors: Zhuanyong Zou E-mail: zouzhy@usx.edu.cn; Guanglei Wu E-mail: wuguanglei@qdu.edu.cn

$$RL = 20 \lg\left(\frac{Z_{in} - Z_0}{Z_{in} + Z_0}\right) \quad (4)$$

where μ_0 and ε_0 represent the complex magnetic parameters and complex dielectric parameters of EMW under vacuum, respectively; μ_r and ε_r are the complex magnetic parameters and complex dielectric parameters of the material, respectively, which can be tested by the vector network analyzer; f is the frequency of EMW; c represents the speed of light in vacuum; d is the thickness of the sample [14–16]. According to the above formula, the thickness of the sample has a crucial impact on its EMW absorption performance. The magnetic loss (tan δ_m) and dielectric loss (tan δ_e) of an absorber can be calculated by its electromagnetic parameters (tan $\delta_m = \mu''/\mu'$, tan $\delta_e = \varepsilon''/\varepsilon'$). The sample's reflection loss (RL) value can be calculated using Eq. (4). The imaginary part (ε'' and μ'') of its electromagnetic parameters reflects the electromagnetic losses caused by the rearrangement of the electric dipole moment and magnetic dipole moment under external electromagnetic fields. In terms of impedance matching, the real and imaginary parts of electromagnetic parameters should exhibit the best electromagnetic matching to achieve the strongest absorption performance [17–19].

The attenuation characteristic is the loss mechanism of EMWs by absorbers after entering the interior. Conductivity loss, multiple reflection and scattering loss mechanism, interface polarization effect, relaxation loss, defect engineering, and eddy current loss can effectively improve the attenuation ability of materials for EMW [20–22]. For example, He *et al.* [23] achieved improved EMW absorption performance by growing polyaniline and ferric oxide on the surface of carbon nanotubes, forming an equivalent cross-linked network. Wang *et al.* [24] constructed a novel carbon cloth@ZnO interface by vertically growing ZnO arrays on the surface of carbon cloth, effectively improving the material's EMW absorption performance. The influence of interface interaction on the material's absorption mechanism was verified through electron holographic imaging analysis to confirm EMW attenuation. Therefore, in the design of a high-performance EMW absorber, the attenuation characteristic and impedance matching must be considered simultaneously. A material's dielectric properties, magnetic behaviors, and microstructure all have a significant impact on its EMW performance, and the synergistic effect of these two factors can significantly enhance the EMW absorption efficiency of absorbers [25–27].

In view of the electromagnetic loss mechanism of EMWs, EMW absorbers can be divided into electrical loss type, magnetic loss type, and electromagnetic synergy type. Electric loss type EMW-absorbing materials mainly attenuate the energy of EMWs through dielectric and conductivity loss and consist of carbon materials (such as graphene, carbon nanotubes, carbon fibers, and graphite), semiconductor oxides or sulfides (such as manganese dioxide, molybdenum disulfide, zinc oxide, and titanium dioxide), and conductive polymers (such as polythiophene, polypyrrole, and polyaniline). Magnetic loss type EMW-absorbing materials mainly consist of ferrite. Electromagnetic synergistic EMW-absorbing materials are currently the most widely reported type; they combine the above two loss mechanisms and can achieve ideal impedance matching by adjusting the component ratio, microstructure, and synthesis process of materials [28–30].

1.2. Ferrites

Ferrite is a composite oxide consisting of iron oxide and one or several other metal oxides (such as $ZnO{\cdot}Fe_2O_3$ and $CoO{\cdot}Fe_2O_3$). Ferrites and their composites have been widely applied in various fields, such as computer, microwave communication, television, automatic control, aerospace, instrumentation, medical, and automotive industries. Ferrites are produced on a large scale in the industry and have a mature production process, which provides broad application prospects for high-performance EMW-absorbing materials based on ferrite. Artificially synthesized ferrites mainly include cobalt ferrite ($CoFe_2O_4$), nickel ferrite ($NiFe_2O_4$), manganese ferrite ($MnFe_2O_4$), strontium ferrite ($SrFe_{12}O_{19}$), and some other multi-element composite ferrite. According to the crystal type, rotary ferrites can be divided into spinel type, garnet type, and magnetite type (hexagonal). Spinel-shaped ferrite, with the chemical formula of MFe_2O_4, has a face-centered cubic structure; its examples include $CoFe_2O_4$ and $NiFe_2O_4$. Magnetite-type ferrite, with the chemical formula of $MF_{12}O_{19}$, has a hexagonal crystal structure similar to natural magnetite; its examples include $BaFe_{12}O_{19}$ and $SrFe_{12}O_{19}$. Garnet-type ferrite possesses a body-centered cubic crystal structure similar to garnet, and its chemical formula is $R_3Fe_5O_{12}$ (one example is $Y_3Fe_5O_{12}$). Compared with other EMW materials, ferrite exhibits the distinct merits of low cost, convenient preparation, and strong magnetic loss. The above three ferrites have been reported in the design of high-performance EMW-absorbing materials [31–35].

1.3. Ferrite-based EMW absorbers

In view of their outstanding magnetic properties, ferrites and their composites have a wide range of applications in EMW absorption. However, ferrites do not possess ideal impedance matching due to their strong magnetic properties and poor conductivity. Zhang *et al.* [36] synthesized large-sized $MnFe_2O_4$ particles under natural conditions via a facile hydrothermal method and subsequently prepared r-GO/$MnFe_2O_4$ nanocomposites with ultrasonic treatment assistance. When the filling ratio of r-Go/$MnFe_2O_4$ composite filler in the PVDF matrix is only 5wt%, the minimum reflection loss (RL_{min}) of r-Go/$MnFe_2O_4$/PVDF can reach −29.0 dB at the frequency of 9.2 GHz, and the bandwidth for frequencies less than −10 dB is 8.00–12.88 GHz. Other ferrite composites, such as PANI/$NiFe_2O_4$@C hybrid [37] and Co-doped NiZn ferrite/graphene nanocomposites [38], were also regarded as ideal EMW absorbers.

The synthesis methods for ferrite can be divided into solid-phase and liquid-phase methods. Solid-phase methods mainly include the high-temperature solid-phase method (HSPM) and self-propagating high-temperature synthesis

method (SHM), both of which complete ferrite preparation by heat treating the solid precursor. Liquid-phase methods mainly include sol–gel method (SGM), coprecipitation method (CCPM), and solvent thermal method (STM). All three complete the binding of metal ions in the liquid phase, but their synthesis techniques differ. Except for SHM, the other four methods are widely applied in the fabrication of high-performance EMW absorption materials. Herein, we will focus on the synthesis of ferrites and their composites and successively introduce the application of these four methods in the preparation of high-performance EMW absorbers [39–41]. This review aims to help researchers understand the advantages and disadvantages of ferrite-based EMW absorbers fabricated through these methods. It also provided important guidance and reference for researchers to design novel high-performance EMW absorption materials based on ferrite.

2. Synthesis methods and EMW absorption performances of ferrite composites

Reported ferrite-based high-performance EMW-absorbing materials are mainly fabricated by HSPM, SGM, CCPM, and STM. We will conduct an in-depth review and analysis of ferrite-based composites synthesized through these four methods from the perspectives of their structures, advantages, disadvantages, EMW-absorbing performances, and absorption mechanisms [42–44].

2.1. Ferrite-based EMW absorbers synthesized via HSPM

HSPM is a traditional method of preparing ferrites. A certain proportion of metal salts or metal oxides are first uniformly mixed; the resulting mixtures are then calcined under high temperature to undergo solid-phase reaction and further ground to obtain uniform-sized ferrite particles. Kozlenko *et al.* [45] uniformly mixed a certain proportion of high-purity Fe_2O_3, ZnO, CuO, and Ga_2O_3 and calcined them at the temperature of 1100°C for 72 h to synthesize $Zn_{0.3}Cu_{0.7}Fe_{1.5}Ga_{0.5}O_4$ polycrystalline ferrite through high-temperature solid-state reaction. Hu *et al.* [46] synthesized $Ni_{0.5}Zn_{0.5}Fe_{2-x}Ti_xO_4$ ferrite using this method and characterized its magnetic properties under room temperature and low temperature. When x was 0.1, the material possessed the strongest magnetic saturation strength, and its magnetic saturation strength at low temperature was significantly higher than that at room temperature. Despite their many advantages, such as easy operation and large-scale production, the ferrites synthesized by HSPM are characterized by relative roughness, structurally uncontrollability, and difficulty in achieving refined synthesis [47].

Owing to drawbacks, including high energy consumption, low conversion rate, insufficient powder size, and easy inclusion of impurities, traditional HSPM has rarely been reported in the design of high-performance EMW absorbers. Some researchers have optimized this method and synthesized EMW-absorbing materials with excellent performance. For example, Feng *et al.* [48] synthesized a set of M-type hexaferrite $Ba_{1-x}Ca_xFe_{12}O_{19}$ ferrites by adopting HSPM with the assistance of polyvinyl alcohol (PVA). $BaCO_3$, Fe_2O_3, and $CaCO_3$ powders with different proportions were first homogeneously dispersed in the PVA matrix, and hexaferrite $Ba_{1-x}Ca_xFe_{12}O_{19}$ ferrite was directly obtained through high-temperature calcination at 1250°C. When x was 0.2, this ferrite achieved the optimum absorption efficiency for EMW, and its RL_{min} reached −31.8 dB. Chen *et al.* [49] adopted polyacrylonitrile as the matrix and iron acetate and cobalt acetate as metal sources and prepared a novel carbon fiber with embedded FeCo/$CoFe_2O_4$ nanoparticles (FeCo/$CoFe_2O_4$/CNFs) by using electrospinning method and high-temperature solid-phase reaction (Fig. 1(a)). The electromagnetic parameters of FeCo/$CoFe_2O_4$/CNFs can be adjusted by controlling the molar ratio of iron and cobalt. When the molar ratio is 7:3, the RL_{min} and effective absorption bandwidth of this composite can reach −18.7 dB and 5 GHz with a sample thickness of only 1.95 mm, respectively. HFSS and radar cross-section (RCS) simulation results showed that when the molar ratio is 9:1, the composite coating achieves good attenuation capability for EMW (Fig. 1(b1)) and its RCS is less than −10 dB (Fig. 1(b2)). When the coating thickness is 1.95 mm, the RCS of FeCo/$CoFe_2O_4$/CNFs can reach up to −34.5 dB (Fig. 1(b3) and (b4)). The interface polarization effect caused by the heterogeneous interface between the FeCo and $CoFe_2O_4$ particles and the carbon material can greatly promote the absorption efficiency of EMWs (Fig. 1(c)). In addition to the abovementioned work, materials with ideal EMW absorption performance, such as $Sr_{0.85}La_{0.15}(MnZr)_xFe_{12-2x}O_{19}$ hexagonal ferrite [50] and hollow strontium ferrite ($SrFe_{12}O_{19}$) nanofiber [51], were fabricated using HSPM with the assistance of polymer. Thus, we consider this strategy effective in promoting HSPM and thereby enhancing the EMW absorption performance.

Structure engineering is an important issue in the design of high-performance EMW absorbers and can effectively improve the EMW absorption performance of ferrites synthesized by HSPM. Li *et al.* [52] designed $ZnFe_2O_4$@PPy microspheres with unique wrinkled core−shell structures using polyvinylpyrrolidone (PVP) through a spray drying method for EMW absorbers. The uniform spherical structure was formed during spray drying, and the PVP was then removed through high-temperature calcination, simultaneously forming wrinkles on the $ZnFe_2O_4$ surface. $ZnFe_2O_4$@PPy microspheres were fabricated using vapor-phase polymerization, and pyrrole monomer vapor was *in situ* grown on the $ZnFe_2O_4$ microsphere wrinkled surface to form a conducive PPy coating shell (Fig. 2(a)–(d)). Owing to their reasonable impedance matching, special structure, and ideal attenuation constant, the RL_{min} and effective absorption bandwidth of $ZnFe_2O_4$@PPy microspheres can reach up to −41 dB and 4.1 GHz, respectively (Fig. 2(e)–(g)). Bulk Ni–Zn ferrite [53] and $TiO_2/Ni_{0.53}Cu_{0.12}Zn_{0.35}Fe_2O_4$ nanocomposites [54] were fabricated via HSPM, and their EMW-absorbing perform-

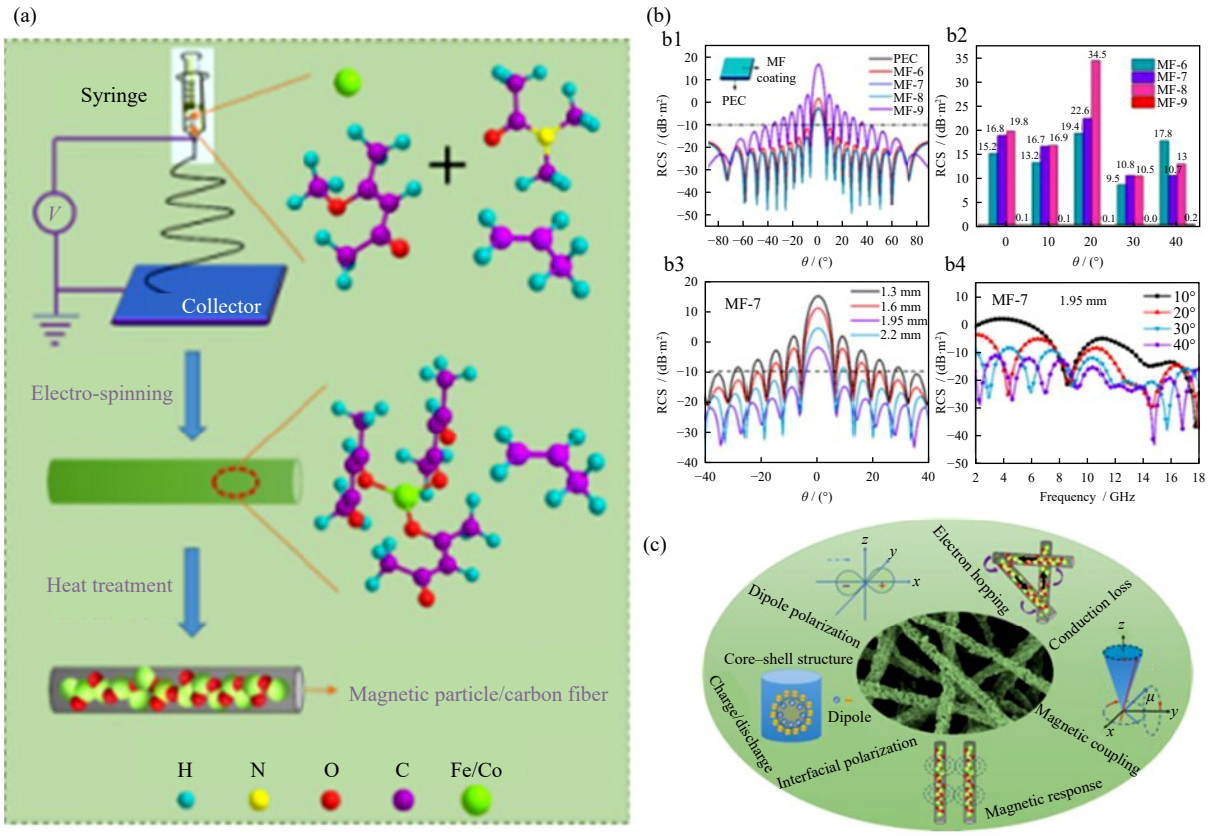

Fig. 1. (a) Fabrication of $FeCo/CoFe_2O_4$/CNFs. HFSS simulation curves (b1) and RCS results (b2) of $FeCo/CoFe_2O_4$/CNF composites with the molar ratio of Fe and Co of 6:4, 7:3, 8:2, and 9:1; RCS results of $FeCo/CoFe_2O_4$/CNF composites with the molar ratio of 7:3 under different thicknesses (b3) and scanning angles (b4). (c) Analysis of the EMW absorption mechanism of $FeCo/CoFe_2O_4$/CNF composites. Reprinted with permission from J.B. Chen, J. Zheng, Q.Q. Huang, *et al.*, *ACS Appl. Mater. Interfaces*, 13, 36182-36189 (2021) [49]. Copyright 2021 American Chemical Society.

ance was significantly enhanced through structural design. Therefore, we believe that the structure engineering of ferrites synthesized by using HSPM is an important research trend to improve their EMW absorption performance and overcome the drawbacks of HSPM.

2.2. Ferrite-based EMW absorbers synthesized via SGM

In addition to solid-phase reaction methods, liquid-phase reaction methods have a wide range of applications in the preparation of ferrites and their composites. SGM is a technique where metal organic or inorganic compounds undergo complete solidification successively through solution, sol, and gel and then form oxides or other compound solids via heat treatment. SGM is a common wet chemical route to prepare materials and has been widely applied to prepare ferrite nanomaterials. Compared with HSPM, SGM requires greatly reduced calcination temperature and is more suitable for the doping of other elements, which can enhance the designability of ferrites [55–57]. In addition, the ferrites synthesized by SGM have a uniform and small particle size, which is beneficial for structural design and functional application. Banerjee *et al.* [58] synthesized a bismuth-doped nickel ferrite spinel ($Ni_{1-x}Bi_xFe_2O_4$) by SGM and found that the material possessed multiferrous properties at room temperature and can be regarded as a temperature memory storage device. Yang *et al.* [59] prepared manganese zinc ferrite ($Mn_\alpha Zn_\beta Fe_{3-\alpha-\beta}O_4$) with uniform hexahedral structure via the sol–gel reaction, and the influence of annealing on the properties of this ferrite was studied in detail. The results indicated that the phase structures and performances of $Mn_\alpha Zn_\beta Fe_{3-\alpha-\beta}O_4$ ferrites were mainly influenced by the protective gas flow rate, heating rate, and temperature during annealing.

SGM plays an important role in the design and preparation of high-performance ferrite-based EMW-absorbing materials. Zhang *et al.* [60] reported a novel Zr^{4+} and Ni^{2+} ion gradient-substituted barium ferrite ($Ba(ZrNi)_{0.6}Fe_{10.8}O_{19}$) with broad EMW absorption bandwidth synthesized through SGM and secondary heat treatment. Characterization results indicated that the frequency range of the barium ferrite doped with Zr^{4+} and Ni^{2+} ions with μ'' larger than 0.3 was broader than that of the original sample. The RL_{min} and EAB width of Zr^{4+} and Ni^{2+} ion gradient-substituted barium ferrite can reach −17.11 dB and 6.24 GHz, respectively, with the sample thickness of 2.8 mm due to the enlarged dielectric and magnetic loss range (Fig. 3). Cheon *et al.* [61] synthesized a Ni–Ti–substituted M-type barium ferrite using citrate SGM and deeply studied its magnetic properties, dielectric properties, and reflection loss curve in the frequency range of 8.2–75 GHz (Fig. 4). The results indicated that the as-synthesized material possessed an RL_{min} of −52 dB at 29.5 GHz with a matching thickness of only 0.95 mm (Fig. 4(b)). Magnetic resonance was considered the most critical factor in en-

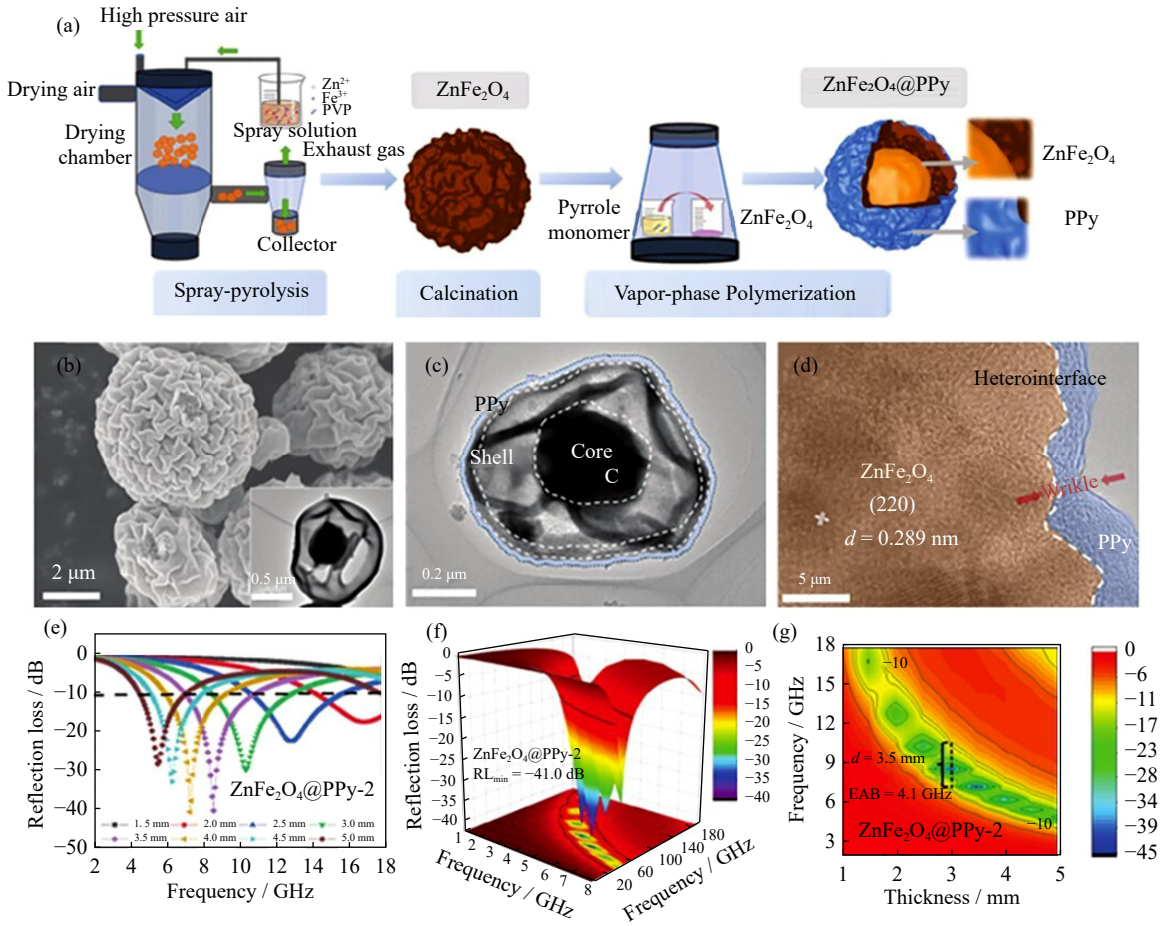

Fig. 2. (a) Synthesis of $ZnFe_2O_4$@PPy microspheres with wrinkled core–shell structure; (b–d) microscopic morphology, structure, and lattice stripe of $ZnFe_2O_4$@PPy, respectively; (e–g) reflection loss (RL) curve of $ZnFe_2O_4$@PPy microspheres. Z.L. Li, H. Zhu, L.J. Rao, *et al.*, *Small*, 20, e2308581 (2024) [52]. Copyright Wiley-VCH GmbH. Reproduced with permission.

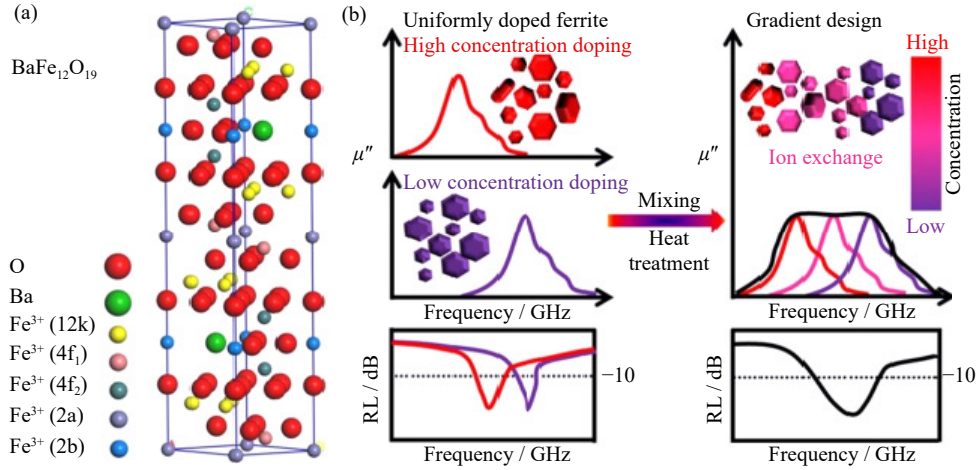

Fig. 3. (a) Crystal structure of barium ferrite; (b) gradient substitution mechanism, and curves of the imaginary part of the dielectric constant and reflection loss of barium ferrite subjected to gradient substitution with Zr^{4+} and Ni^{2+} ions [60]. Reprinted from *Ceram. Int.*, 46, Y.T. Zhang, C.Y. Liu, K.S. Peng, et al., Synthesis of broad microwave absorption bandwidth Zr^{4+}–Ni^{2+} ions gradient-substituted barium ferrite, 25808-25816, Copyright 2020, with permission from Elsevier.

hancing the EMW absorption performance of this material (Fig. 4(c)). In addition to the above materials, Sr-doped $YFeO_3$ ($Y_{1-x}Sr_xFeO_3$) [62], $Ni_{0.5}Zn_{0.5}Fe_2O_4/SrFe_{12}O_{19}$ composites [63], and polyaniline/$NiFe_2O_4$/graphite nanosheet composites (PANI/$NiFe_2O_4$/GN) [64] were synthesized via SGM.

Although the ferrite synthesized using SGM possesses a series of advantages, such as strong magnetic properties, good chemical uniformity and high purity, its microstructure is difficult to control and design, especially at the nanoscale. EMW absorption efficiency is mainly determined by the impedance matching and attenuation characteristics. The micro-

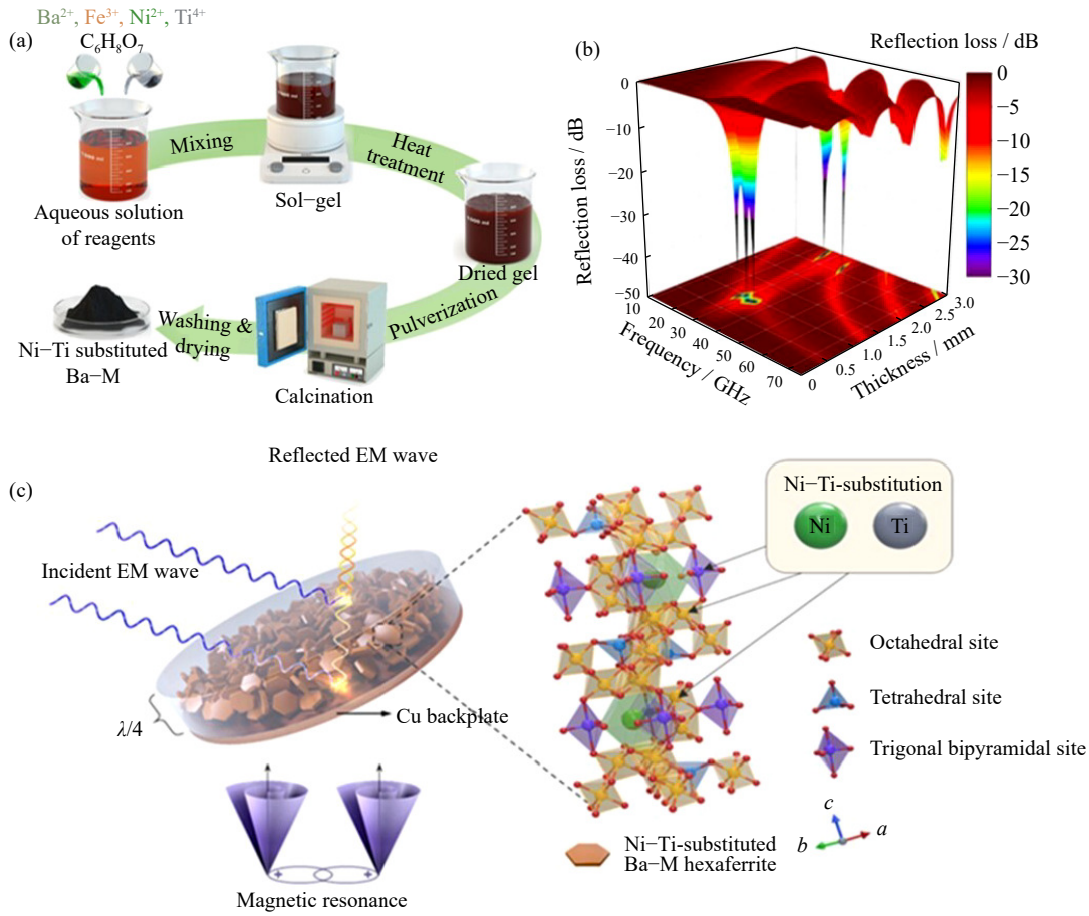

Fig. 4. (a) Synthesis, (b) reflection loss curve, and (c) EMW absorption mechanism of Ni–Ti-substituted Ba–M ferrite [61]. Reprinted from *J. Alloy. Compd.*, 976, S.J. Cheon, J.R. Choi, S.B. Lee, *et al.*, Frequency tunable Ni–Ti-substituted Ba–M hexaferrite for efficient electromagnetic wave absorption in 8.2–75 GHz range, 173019, Copyright 2024, with permission from Elsevier.

structure of materials has a significant impact on the attenuation characteristics of EMW. The poor designability of the ferrite synthesized via SGM would seriously limit its application prospects in the development of high-performance EMW absorption materials. This ferrite also has other defects, such as high energy consumption and great harm to the environment when using metal nitrates [65–67]. Thus, we must consider designing the microstructure of ferrite synthesized via SGM in the nanometer size to enhance the EMW-absorbing performance.

2.3. Ferrite-based EMW absorbers synthesized via CCPM

As a typical liquid-phase method, CCPM is also a traditional and effective approach for preparing ferrite. It uses precipitants (such as OH^- and CO_3^{2-}) to coprecipitate metal ions in the solution. The product is obtained through processes including filtration, washing, drying, and burning. CCPM possesses a series of advantages such as simple operation, low cost, good crystal structure of the prepared ferrite, uniform size, and easy industrial production. However, the solubility of metal ions in solution can limit the performance and reaction yield of the synthesized ferrite [68]. Aoopngan *et al.* [69] successfully synthesized amine-functionalized $MgFe_2O_4$ nanoparticles ($MgFe_2O_4$–NH_2NPs) using ethanolamine as a surface modifier through a coprecipitation reaction. Magnetic characterization results indicated that the synthesized functionalized ferrite nanoparticles have superparamagnetism and extremely high magnetic saturation strength and can be used as reusable magnetic adsorbents for removing Congo red. Iranmanesh *et al.* [70] fabricated nickel ferrite particles with a size of less than 10 nm using iron chloride and nickel chloride as raw materials through an original one-step precipitation method. The effect of reaction pH on the microstructure and magnetic properties of nickel ferrite was also studied in depth. Many other ferrite-based composites, such as $CoFe_2O_4$-reduced graphene oxide nanocomposites [71] and $Ni_{0.5}Cu_{0.5}Fe_2O_4$ nanoparticles [72] were prepared via CCPM.

Compared with HSPM and SGM, CCPM can be adopted to flexibly design the microstructure of high-performance EMW-absorbing materials during preparation. An effective strategy is to grow ferrite on the surface of 2D materials to form ideal impedance matching, thus enhancing the EMW absorption performance. Lei *et al.* [73] adopted CCPM to fabricate Co-doped NiZn ferrite/polyaniline/MXene composite hybrid materials ($Ti_3C_2T_X$/CNZFO/PANI) with broad and high-performance EMW absorption capacity. The Co-doped NiZn ferrite particles and PANI molecular chains were homogeneously grown between $Ti_3C_2T_X$ sheets, forming a novel sandwich-like structure (Fig. 5(a)). The RL_{min} of this

composite can reach −37.1 dB with a sample thickness of 2.2 mm (Fig. 5(b) and (c)), which can mainly be attributed to the eddy current loss, natural resonance, interfacial polarization, dipole polarization, and multiple reflections of the layered structure. Chen *et al.* [74] designed a novel one-pot reaction to synthesize molybdenum disulfide@nitrogen-doped carbon decorated with ultrasmall $CoFe_2O_4$ particles with quantum size (MoS_2@NC@$CoFe_2O_4$). Chemical coprecipitation carried out at high temperatures greatly reduces the size distribution of $CoFe_2O_4$ particles (less than 10 nm). Owing to the reasonable impedance matching, multiple reflections and losses, and interface polarization, the RL_{min} and EAB width of MoS_2@NC@$CoFe_2O_4$ can reach −46.7 dB and 3.5 GHz, respectively (Fig. 6). Many other ferrite/2D material composites such as $NiFe_2O_4$-decorated poly(3, 4-ethylenedioxythiophene)/graphene (RGO/PT@$NiFe_2O_4$) [75] and graphene@PANI@porous TiO_2 composites (RGO@PANI@TiO_2) [76] were successfully synthesized as high-performance EMW absorbers via CCPM, indicating that it is an effective strategy.

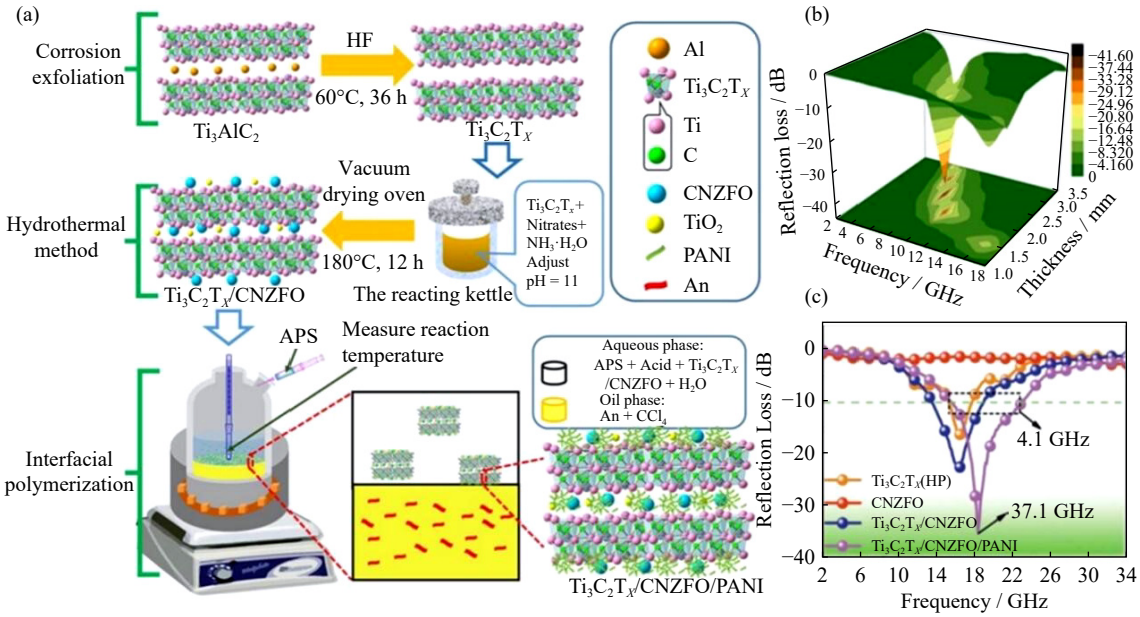

Fig. 5. (a) Synthesis procedure and (b) reflection loss curve of $Ti_3C_2T_X$/CNZFO/PANI composite; (c) reflection loss curves of $Ti_3C_2T_X$ and CNZFO composites [73]. Reprinted from *Ceram. Int.*, 46 Y.M. Lei, Z.J. Yao, S.Z. Li, *et al.*, Broadband high-performance electromagnetic wave absorption of Co-doped NiZn ferrite/polyaniline on MXenes, 10006-10015, Copyright 2020, with permission from Elsevier.

Another important strategy is to design or modify the structure of ferrite by CCPM, which can effectively enhance EMW absorption performance. Zhou *et al.* [77] designed a new flower-like $ZnFe_2O_4$ ferrite-loaded graphene (3D-ZFO/GNs) via CCPM. The coprecipitation of iron ions and zinc ions in an alkaline solution transforms the 3D-flower-like zinc oxide template composed of flakes into zinc ferrite composed of lines (Fig. 7(a)). The EAB width of 3D-ZFO/GNs can reach 5.56 GHz with a sample thickness of only 1.5 mm, which can be attributed to the reasonable impedance matching, magnetic resonance, polarization effect, and heterojunction interface between the flower-like $ZnFe_2O_4$ and graphene (Fig. 7(b) and (c)). Zheng *et al.* [78] successfully synthesized novel snowflake-shaped and nanoflower-shaped Cu_xS/$CoFe_2O_4$ composites by regulating different metal salts and solvents via CCPM and solvent thermal reaction (Fig. 8(a)–(d)). After the proportion of electromagnetic components of Cu_xS and $CoFe_2O_4$ was adjusted, the RL_{min} and EAB width of the nanoflake-shaped sample reached −57.6 dB and 4.0 GHz, respectively. With the microscopic morphology changes to its snowflake shape, the RL_{min} and EAB width of the Cu_2S/$CoFe_2O_4$ sample increased to −66.58 dB and 6.64 GHz, respectively, when the sample thickness was 2.1 mm (Fig. 8(e)). Factors including magnetic resonance effect, eddy current loss, interface polarization, conductivity loss, multiple reflections, and scattering all contribute to the attenuation of EMWs (Fig. 8(f)).

Compared with HSPM and SGM, CCPM possesses many advantages in the design of high-performance EMW-absorbing materials. First, CCPM broadens the designability of the ferrite microstructure. We can obtain ferrites with different sizes and structures by controlling the reaction conditions and synthesis process. Second, CCPM is conducive to obtaining ferrite composites or modifying other materials, which is helpful in constructing heterogeneous interfaces [79–81]. Finally, the application of CCPM to synthesize ferrite is suitable for regulating the dielectric and magnetic parameters of its composites, forming the best impedance matching and enhancing their EMW absorption performance. CCPM requires lower calcination temperature than the former two methods and does not even necessitate a high-temperature treatment. However, the production and magnetic properties of ferrites obtained via CCPM are inferior to those prepared by HSPM and SGM due to the solubility of metal ions and the hydroxides of metals [82–84].

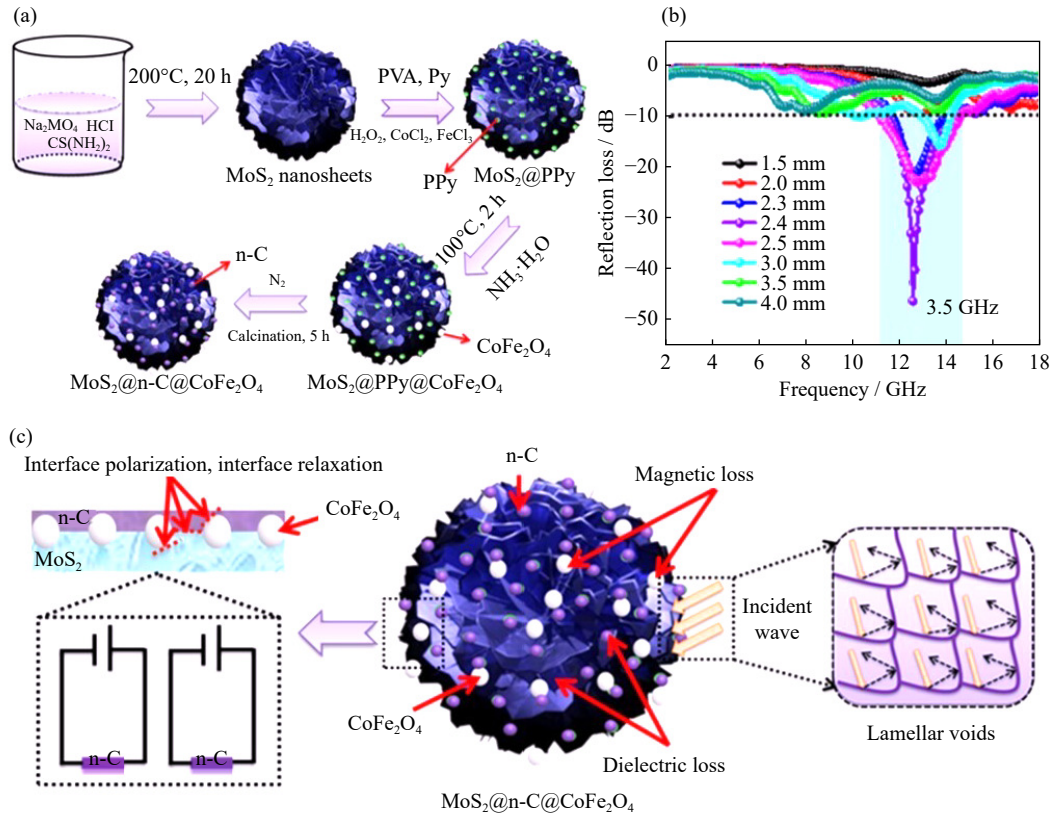

Fig. 6. (a) Fabrication procedure, (b) reflection loss curves, and (c) EMW absorption mechanism of MoS_2@NC@$CoFe_2O_4$ [74]. Reprinted from *Carbon*, 163, X.L. Chen, W. Wang, T. Shi, *et al.*, One pot green synthesis and EM wave absorption performance of MoS_2@nitrogen doped carbon hybrid decorated with ultrasmall cobalt ferrite nanoparticles, 202-212, Copyright 2020, with permission from Elsevier.

2.4. Ferrite-based EMW absorbers synthesized via STM

STM, another liquid-phase method, causes the metal salts in the solvent to crystallize and grow due to supersaturation under high temperature and pressure conditions, thereby obtaining ferrite. The ferrite prepared by this method exhibits many merits, such as high purity, good crystallinity, and ideal magnetic properties. However, compared with other methods, STM must be carried out in the reactor, and the solvent after the reaction is difficult to recycle or post-treat, which greatly increases its cost. Therefore, the large-scale industrial application of this method is difficult to realize. The selected solvent, reaction temperature, and heating rate have a significant impact on the morphology and performance of the synthesized ferrite [85–87]. Therefore, changing these reaction conditions can optimize the experiment and achieve controllable reactions. Chu *et al.* [88] first prepared nickel ferrite ($NiFe_2O_4$) with a uniform hollow cubic structure using iron bimetallic organic framework (Ni–Fe MOF) as raw materials through a one-step solvent thermal reaction. Nickel cobalt layered double hydroxide (Ni Co LDH) nanowires were then combined with reduced graphene oxide (r-GO) through a thermal decomposition reaction to form a layered nickel ferrite@nickel cobalt nanowire@graphene composite cubic structure ($NiFe_2O_4$–NiCo–LDH@rGO). This layered hollow structure significantly increases the contact area between the material and electrolyte, thereby enhancing the electrochemical performance. $CoFe_2O_4$/CNT nanocomposites [89], hierarchically porous r-GO/MnZn ferrite composites [90], and PMMA-modified $MnFe_2O_4$ polyaniline nanocomposites [91] were all fabricated by using STM. At present, STM is the most widely used technique for the synthesis of high-performance EMW absorption materials.

CCPM and STM are both liquid-phase synthesis methods and thus have many similarities, such as low cost, good crystal structure of the prepared ferrite, uniform size, and simple operation. Compared with those obtained by CCPM, the microstructure and morphology of ferrite synthesized by STM are more uniform. The ferrites and their composites synthesized by STM have greater flexibility in structural design at the nanoscale [92]. Chai *et al.* [93] adopted a solvent thermal reaction to fabricate a novel $ZnFe_2O_4$@porous hollow carbon microsphere ($ZnFe_2O_4$@PHCMS); the $ZnFe_2O_4$ nanospheres were *in-situ* grown inside hollow carbon microspheres by self-assembly. The RL_{min} of the $ZnFe_2O_4$@PHCMS sample reached −51.43 dB at 7.2 GHz with a sample thickness of 4.8 mm (Fig. 9(a)). Chen *et al.* [94] designed a series of interconnected magnetic carbon@$Ni_xCo_{1-x}Fe_2O_4$ nanospheres (C@$Ni_xCo_{1-x}Fe_2O_4$) with a core-shell structure by STM. When the x value was 0.75, C@$Ni_xCo_{1-x}Fe_2O_4$ possessed optimum absorption efficiency for EMW; its RL_{min} and EAB width reached −51 dB and 3.3 GHz, respectively, with the sample thickness of only 1.9 mm (Fig. 9(b)). Guo *et al.* [95] synthesized unique dual-loss $Ti_3C_2T_x$ MXene/$Ni_{0.6}Zn_{0.4}Fe_2O_4$ heterogeneous nano-

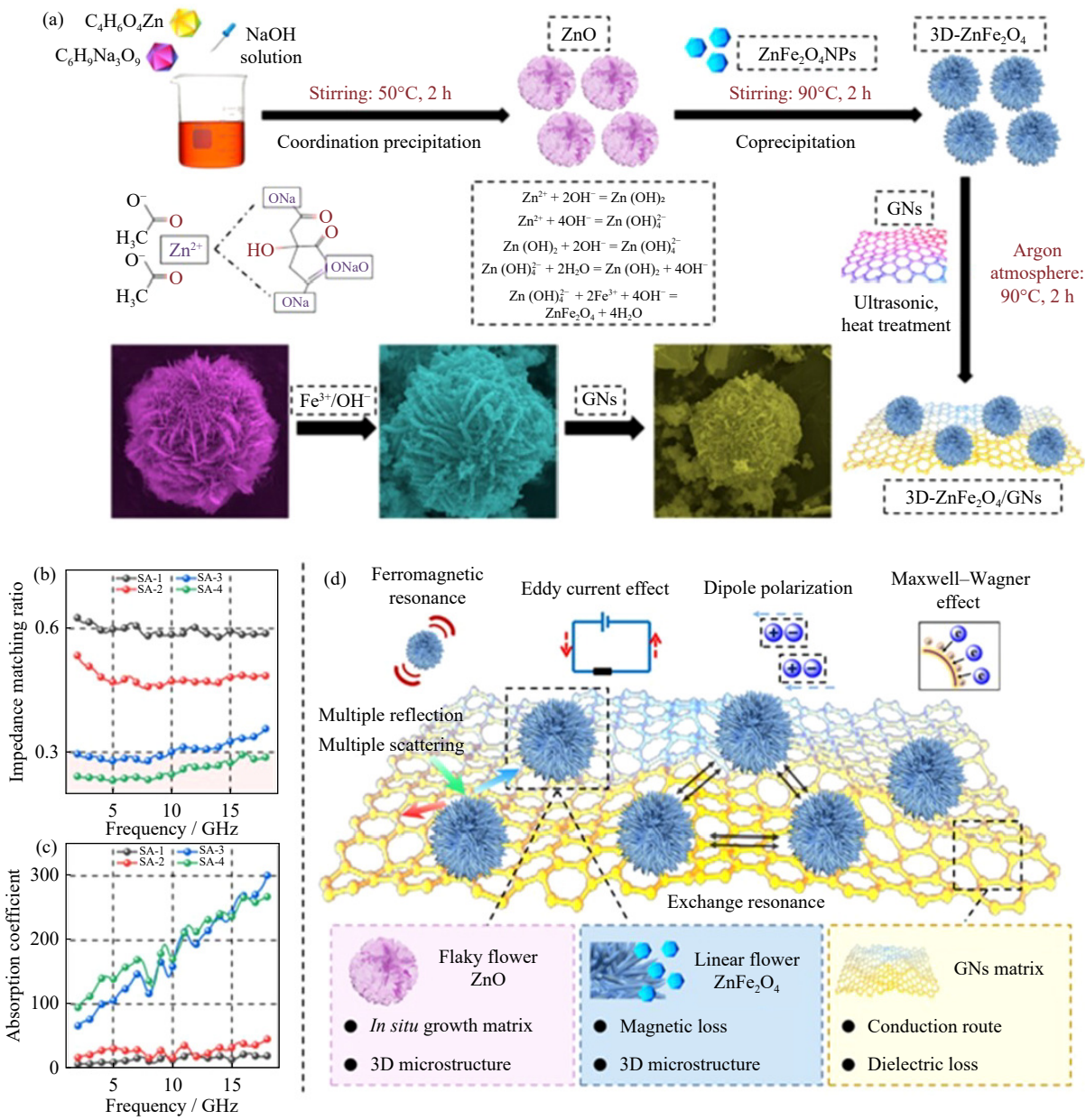

Fig. 7. (a) Synthesis procedure, (b) impedance matching ratio, (c) attenuation constant (α), and (d) EMW absorption mechanism of 3D-ZFO/GNs [77]. Reprinted from *J. Alloy. Compd.*, 889, J.T. Zhou, B. Wei, M.Q. Wang, *et al.*, Three dimensional flower like $ZnFe_2O_4$ ferrite loaded graphene: Enhancing microwave absorption performance by constructing microcircuits, 161734, Copyright 2021, with permission from Elsevier.

composites (MXene/NZFO) by incorporating. $Ni_{0.6}Zn_{0.4}Fe_2O_4$ nanoparticles onto the surface and between the layers of MXene via a straightforward in-situ hydrothermal method (Fig. 9(c)). Owing to the synergy effect of magnetic loss and dielectric loss, the material possesses an RL_{min} of −66.2 dB at 15.2 GHz. In summary, STM has been widely used in the design and synthesis of high-performance EMW absorbers. We can design the structure of ferrite composites through solvent thermal reactions to effectively enhance their EMW absorption performance.

Owing to the high flexibility of STM, it has significant advantages for the structural design and morphology control of high-performance EMW-absorbing materials. Hollow structural design is an important research direction in EMW absorbers and is beneficial for achieving a light weight, increasing the specific surface area, and promoting the synergistic effect of multiple loss mechanisms. STM has been widely applied in the design of high-performance EMW-absorbing materials with a hollow structure [96]. Ge *et al.* [97] constructed a novel hierarchical $CoFe_2O_4$/CoFe@C microsphere with a hollow structure through STM, self-sacrifice processing, and carbon calcination (Fig. 10(a)). Part of the $CoFe_2O_4$ nanoparticles were reduced to CoFe alloys under high temperature with encapsulated carbon, simultaneously forming oxygen vacancies (Fig. 10(b)). After its structure and electromagnetic performance were optimized, the RL_{min} of the $CoFe_2O_4$/CoFe@C sample reached −51 dB at a filled ratio of 30wt%. Meanwhile, its EAB width was 5.19 GHz with a thickness of 2.17 mm, indicating that the material possesses excellent absorption capacity for EMW. Its unique

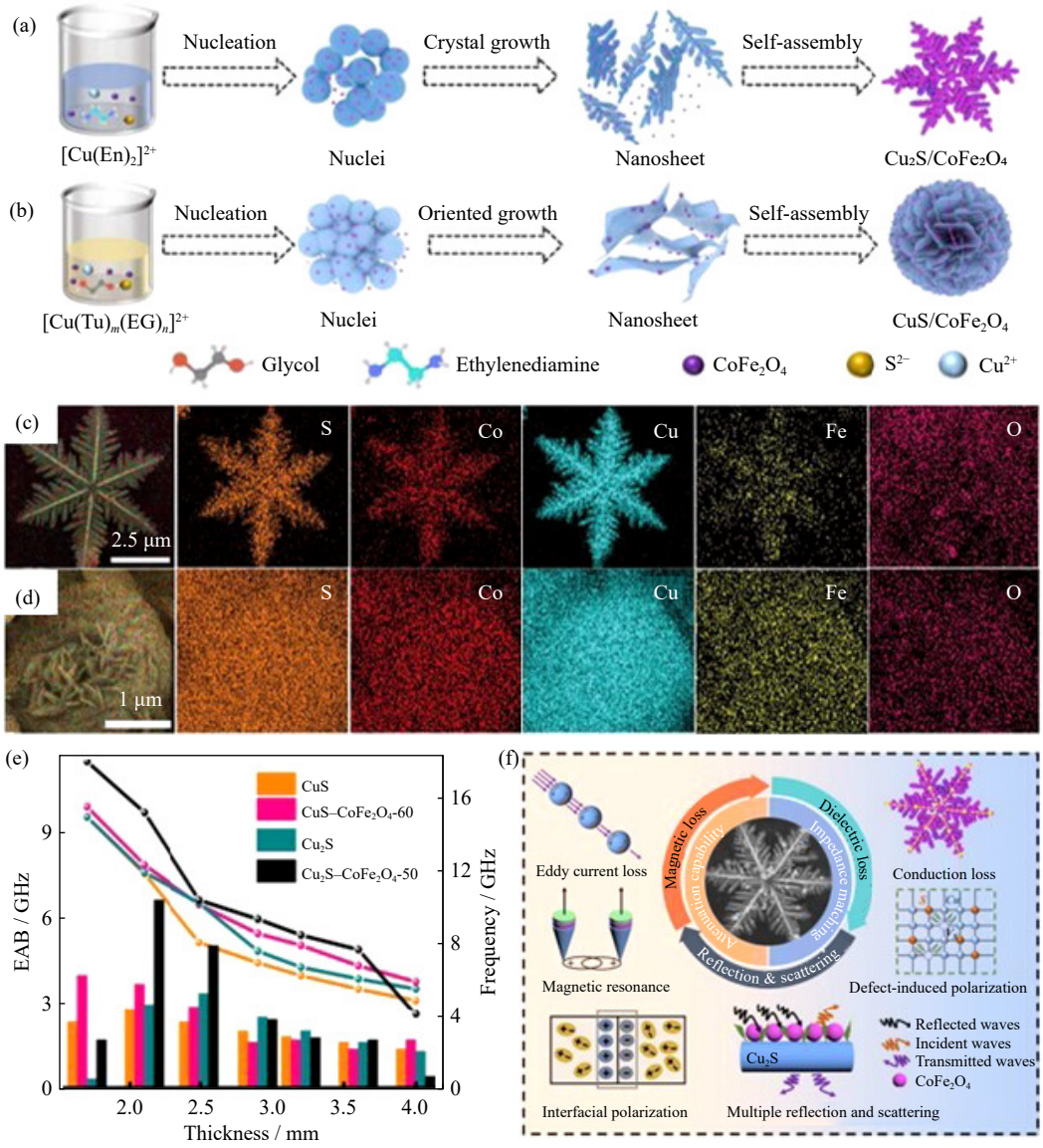

Fig. 8. (a, b) Synthesis, (c, d) microscopic morphology and chemical element composition of $Cu_xS/CoFe_2O_4$ composites, (e) EAB widths of Cu_xS and $Cu_xS/CoFe_2O_4$ composites, and (f) EMW absorption mechanism of $Cu_xS/CoFe_2O_4$ composites [78]. Reprinted from *Chem. Eng. J.*, 457, T.T. Zheng, Y. Zhang, Z.R. Jia, *et al.*, Customized dielectric-magnetic balance enhanced electromagnetic wave absorption performance in $Cu_xS/CoFe_2O_4$ composites, 140876, Copyright 2023, with permission from Elsevier.

hollow and layered structure is a key factor in enhancing its EMW absorption (Fig. 10(c) and (d)). Zhang *et al.* [98] designed Co–$CoFe_2O_4$ coated hollow mesoporous carbon spheres (Co–$CoFe_2O_4$@PCHMs) via the *in situ* growth of Co–$CoFe_2O_4$ crystals on the surface of hollow mesoporous carbon spheres during solvent thermal reaction (Fig. 11(a) and (c)). The RL_{min} of Co–$CoFe_2O_4$@PCHMs can reach −65.31 dB when the thickness is 2.1 mm (Fig. 11(b)). When EMWs are incident on the interior of composite microspheres, they undergo multiple reflections and scattering, resulting in energy attenuation (Fig. 11(d)). Other factors such as conductivity loss, interface polarization, dipole polarization, and resonance effect also have a synergistic effect on EMW absorption. Designing hollow structures is an effective strategy to improve the EMW absorption performance of materials. For example, nickel-magnesium ferrite-decorated nitrogen-doped graphene aerogel (NRGO/$Ni_{0.5}Mg_{0.5}Fe_2O_4$) [99] and nickel ferrite/graphite nanosheet ($NiFe_2O_4$/GN) [100] ferrite-based composites with hollow structures were prepared via STM and showed excellent EMW absorption performance.

The development of innovative solvent thermal synthesis techniques for preparing high-performance EMW-absorbing materials based on ferrite is another hot research issue. Liu *et al.* [101] designed a novel bi-ion synergistic regulation strategy to fabricate hollow FeCo/$CoFe_2O_4$ microspheres for EMW absorbers. NH_4F controlled the nucleation and structural formation during the solvent thermal process. The novel structure of FeCo/$CoFe_2O_4$ microspheres can be attributed to the dynamic cycles between the metal complexes and precipitates, which results from the coordination etching effects of F^- and the hydrolysis-complex contributions of NH_4^+ (Fig. 12(a)–(c)). The microstructure, structure, and electromagnetic parameters of FeCo/$CoFe_2O_4$ microspheres can be con-

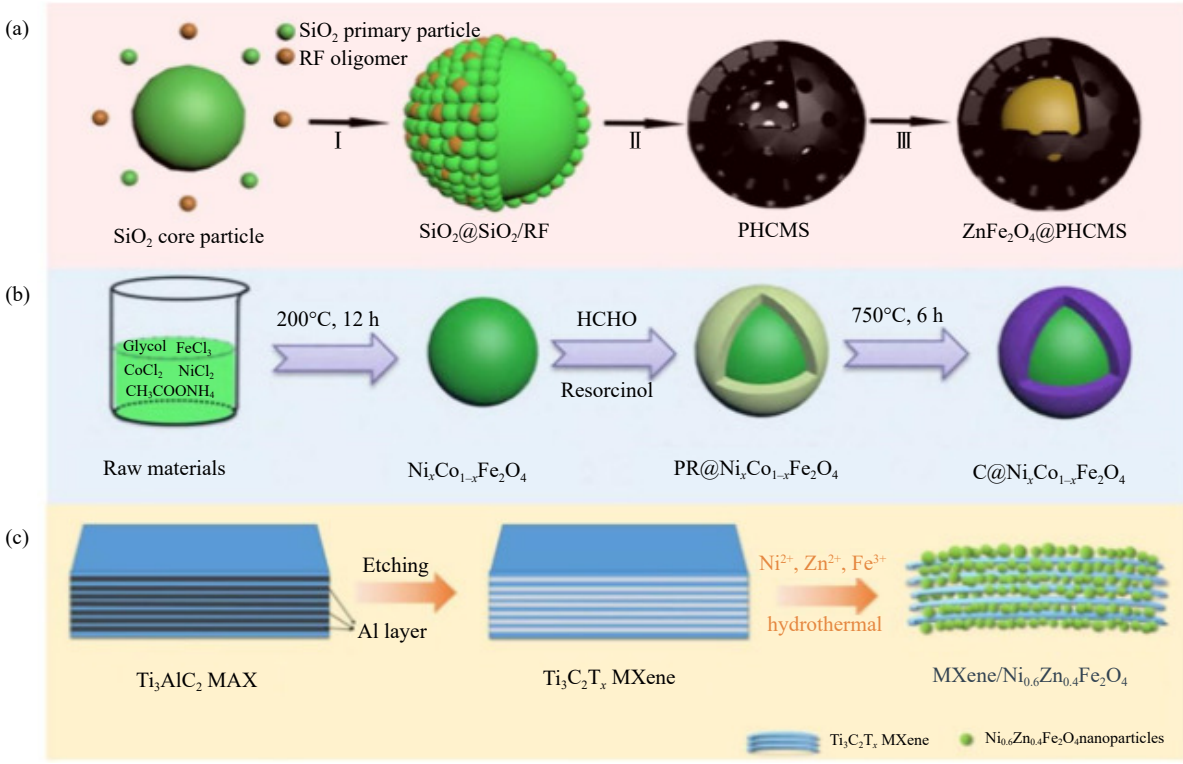

Fig. 9. (a) Synthesis of $ZnFe_2O_4$@PHCMS [93], (b) C@$Ni_xCo_{1-x}Fe_2O_4$ [94], and (c) MXene/NZFO [95]. (a) Reprinted from *J. Colloid Interface Sci.*, 581, L. Chai, Y.Q. Wang, N.F. Zhou, *et al.*, *In-situ* growth of core–shell $ZnFe_2O_4$ @ porous hollow carbon microspheres as an efficient microwave absorber, 475-484, Copyright 2021, with permission from Elsevier. (b) Reprinted from *J. Colloid Interface Sci.*, 606, X.L. Chen, Y. Wang, H.L. Liu, *et al.*, Interconnected magnetic carbon@$Ni_xCo_{1-x}Fe_2O_4$ nanospheres with core–shell structure: An efficient and thin electromagnetic wave absorber, 526-536. Copyright 2022, with permission from Elsevier. (c) Reprinted from *J. Alloy. Compd.*, 887, S.Y. Guo, H.L. Guan, Y. Li, *et al.*, Dual-loss $Ti_3C_2T_x$ MXene/$Ni_{0.6}Zn_{0.4}Fe_2O_4$ heterogeneous nanocomposites for highly efficient electromagnetic wave absorption, 161298, Copyright 2021, with permission from Elsevier.

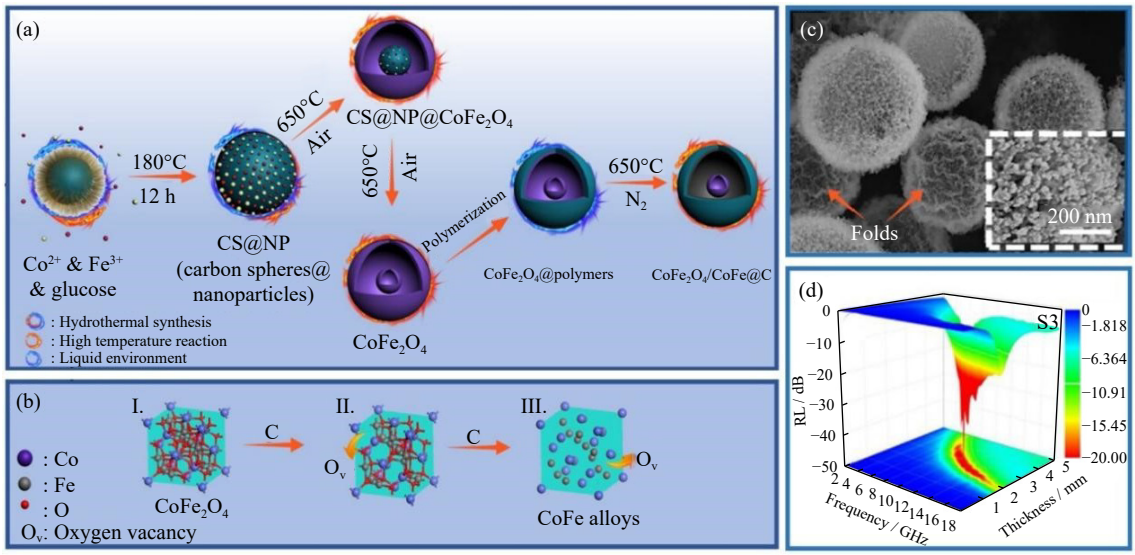

Fig. 10. (a) Preparation of $CoFe_2O_4$/CoFe@C microsphere; (b) specific crystal transformation and the formation of $CoFe_2O_4$ composites; (c) microscopic morphology and structure and (d) reflection loss curve of $CoFe_2O_4$/CoFe@C composite [97]. Reprinted from *J. Mater. Sci. Technol.*, 81, J.W. Ge, S.M. Liu, L. Liu, *et al.*, Optimizing the electromagnetic wave absorption performance of designed hollow $CoFe_2O_4$/CoFe@C microspheres, 190-202, Copyright 2021, with permission from Elsevier.

trolled by adjusting the NH_4F addition amount (Fig. 12(d)). After the synthesis process was optimized, the FeCo/CoFe_2O_4 sample possessed an RL_{min} of −55.6 dB with a sample thickness of only 1.3 mm (Fig. 12(e)). The sample's electronic holographic reconstruction maps revealed extensive coupling of neighboring 3D microspheres, with minor magnetic coupling originating from 0D nanoparticles, which can be attributed to the special hollow structure. Thus, magnetic coupling is beneficial for improving the EMW absorption capacity of materials (Fig. 12(f) and (g)).

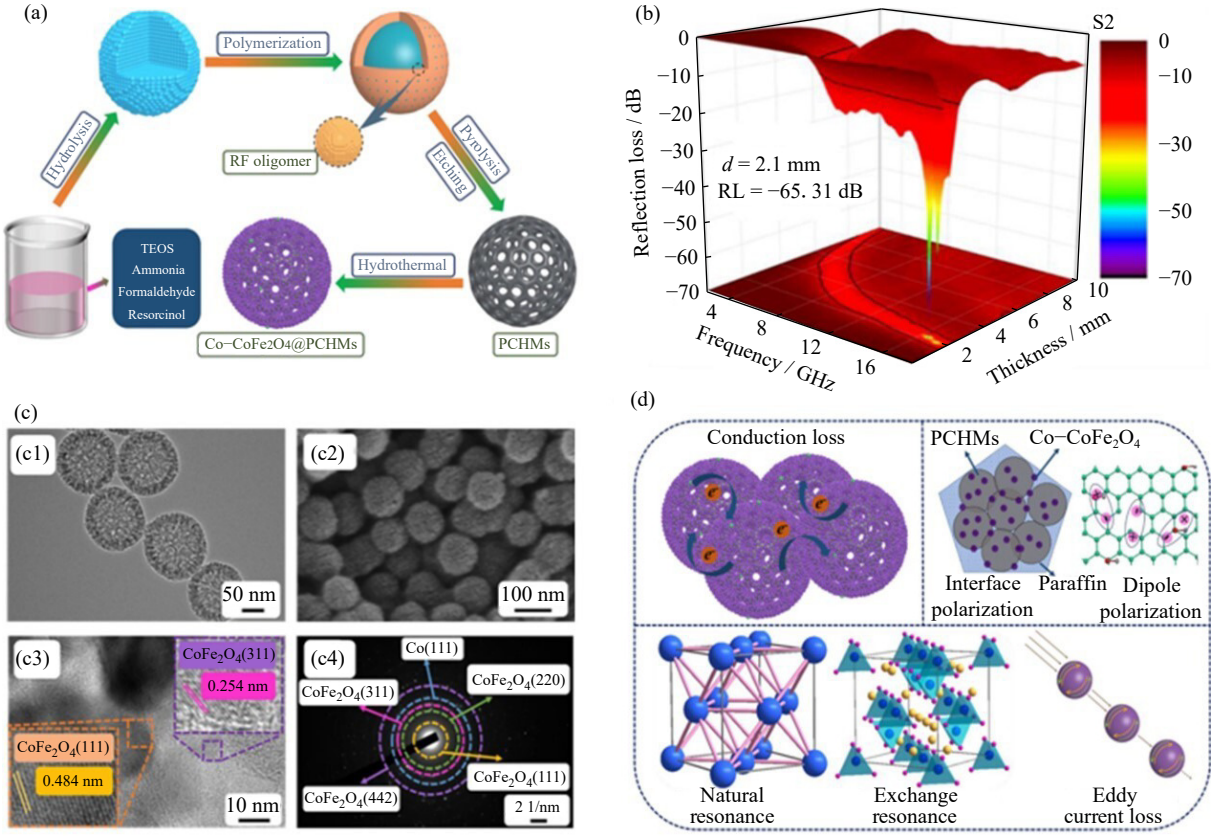

Fig. 11. (a) Synthesis, (b) reflection loss curve, (c) microscopic morphology, and (d) absorption mechanism for EMW of Co–$CoFe_2O_4$@PCHMs [98]. Reprinted from *Chem. Eng. J.*, 421, H.X. Zhang, Z.R. Jia, B.B. Wang, *et al.*, Construction of remarkable electromagnetic wave absorber from heterogeneous structure of Co–$CoFe_2O_4$@mesoporous hollow carbon spheres, 129960, Copyright 2021, with permission from Elsevier.

Huang *et al.* [102] adopted a confined growth strategy during solvent thermal reaction to fabricate bi-metal MOF-derived $ZnFe_2O_4$–ZnO–Fe@C microspheres (ZZFC) with heterogeneous interfaces. 2-Methylimidazole acted as the complexing agent of Fe^{2+} and Zn^{2+}, simultaneously forming the FeZn–ZIF precursor, which was then calcined under hydrogen/argon atmosphere to obtain $ZnFe_2O_4$–ZnO–Fe@C microspheres (Fig. 13(a)). The RL_{min} of $ZnFe_2O_4$–ZnO–Fe@C microspheres can reach up to −66.5 dB when the sample thickness is 2.0 mm (Fig. 13(b) and (c)). At this thickness, RCS simulation results indicated that the sample's RCS was less than −20 dB·m^2 within the range of $-90° < \theta < -9°$ and $9° < \theta < 90°$. Reasonable impedance matching (Fig. 13(d)) and the synergistic effect of electric dipole polarization, interface polarization, and magnetic coupling are considered the main factors contributing to this material's excellent EMW absorption performance (Fig. 13(e)). In addition to the above research work, superior EMW absorbers such as core-shell $CoFe_2O_4$@PPy nanoparticles with reduced graphene oxide ($CoFe_2O_4$@PPy-rGO) [34], MoS_2/$CuFe_2O_4$ nanocomposite [103], and $ZnFe_2O_4$-decorated carbon cloth ($ZnFe_2O_4$/CC) [104] were fabricated via innovative solvent thermal synthesis techniques. Except for the above issues, we consider that the flexible construction of heterogeneous interfaces, regulation of impedance matching, and control of synthetic costs are worthy of in-depth research issues when developing ferrite-based high-performance EMW absorbers through STM.

3. Summary

The synthesis methods of ferrites can be divided into solid-phase and liquid-phase methods. Solid-phase methods mainly include HSPM and HSM, both of which complete ferrite preparation by heat treating the solid precursor. Liquid-phase methods mainly include SGM, CCPM, and STM. All three methods complete the binding of metal ions in the liquid phase. Except for HSM, the other four methods are all widely applied in the fabrication of high-performance EMW absorption materials. Among them, HSPM shows drawbacks, such as uncontrollable structure and size and high energy consumption. Therefore, polymers (such as PVA, PVP, and PAN) are adopted as regulators to enhance the materials' EMW absorption performance. For SGM, the poor designability has seriously limited its application prospects in the development of high-performance EMW absorption materials. Thus, we consider designing the microstructure of ferrites on the nanometer scale to enhance the EMW absorption performance. Compared with HSPM and SGM, CCPM can be adopted to flexibly design the microstructure of high-performance EMW-absorbing materials during preparation and does not even require high-temperature treatment. In addition, the required calcination temperature of CCPM is lower than that of the former two methods. However, limited by the

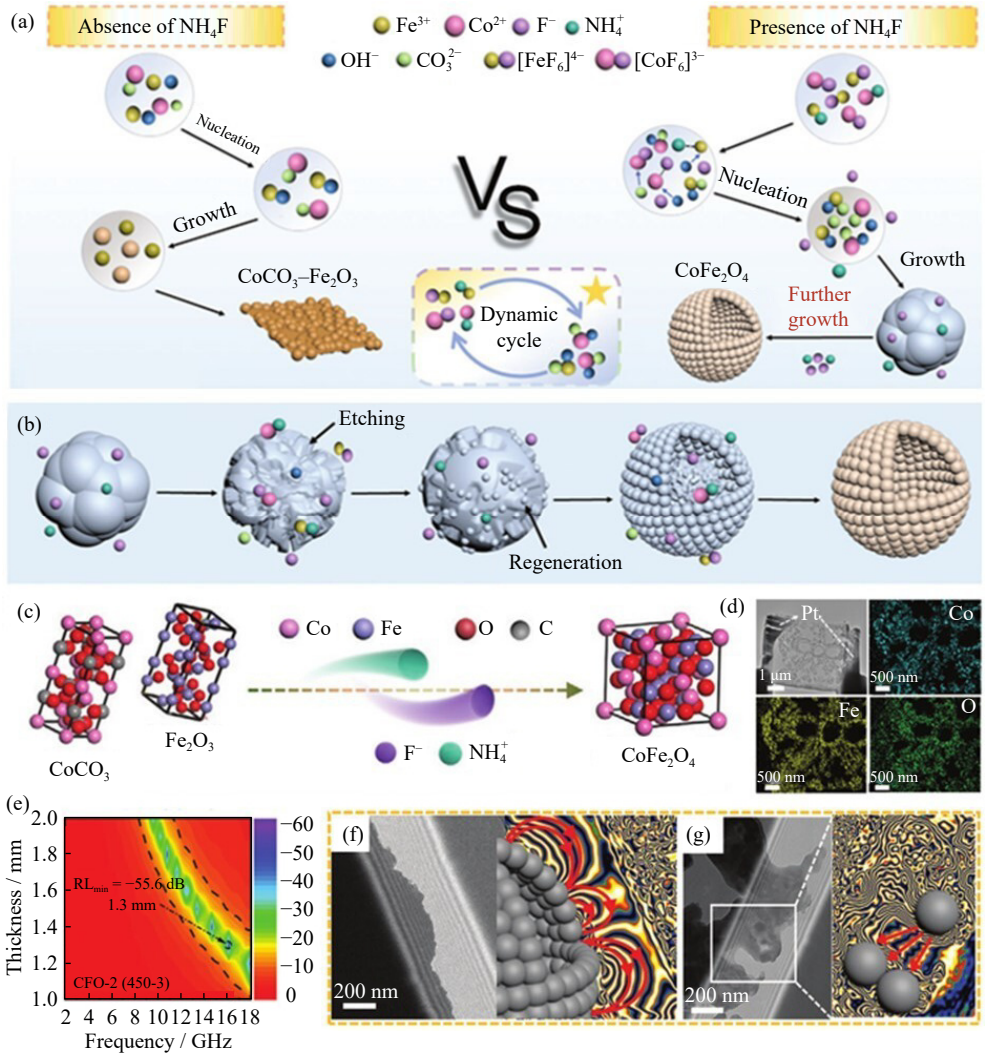

Fig. 12. (a, b) Synthesis, (c) mechanism, (d) microscopic morphology and chemical element composition, and (e) reflection loss curve of FeCo/$CoFe_2O_4$ microspheres; (f, g) holograms and corresponding magnetic lines for the flux distribution maps of FeCo/$CoFe_2O_4$ microspheres. M. Liu, B. Zhao, K. Pei, *et al.*, *Small*, 19, 2300363 (2023) [101]. Copyright Wiley-VCH GmbH. Reproduced with permission.

solubility of metal ions and the hydroxides of metals, the production and magnetic properties of the ferrites obtained via CCPM are inferior to those of the ferrites fabricated via HSPM and SGM. Compared with CCPM, STM provides ferrites with more uniform microstructure and morphology. STM provides great flexibility in the structural design of ferrites and their composites at the nanoscale, which is beneficial for improving EMW absorption performance. The specific EMW absorption performances of the above ferrite-based materials fabricated via HSPM, SGM, CCPM, and STM are summarized in Table 1.

4. Conclusions and prospect

In this review, we introduced four commonly used synthesis methods, namely, HSPM, SGM, CCPM, and STM, for ferrites and their composites in detail. We also analyzed their advantages and disadvantages in the design and fabrication of ferrite-based high-performance EMW absorbers. The conclusions and research prospects are as follows.

(1) Polymer assistance is an effective strategy to promote HSPM, thereby enhancing the EMW absorption performance.

(2) The structural design of ferrite composites synthesized via SGM at the nanoscale is an important issue and can effectively enhance the materials' EMW-absorbing capacity.

(3) Construction of heterogeneous interface, design of hollow structure, and regulation of impedance matching are common strategies for improving the EMW absorption performance of ferrite-based materials fabricated by CCPM and STM.

(4) Developing innovative solvent thermal synthesis techniques is an effective approach for preparing novel high-performance EMW absorbers. MOF-derived ferrite composites possess broad research prospects for EMW absorbers.

(5) EMW absorbers based on rare earth element-doped ferrite, the application of ferrite composites in stealth coating, and the design of multifunctional ferrite-based EMW-absorbing materials are important issues in future research.

This review aims to help researchers understand the ad-

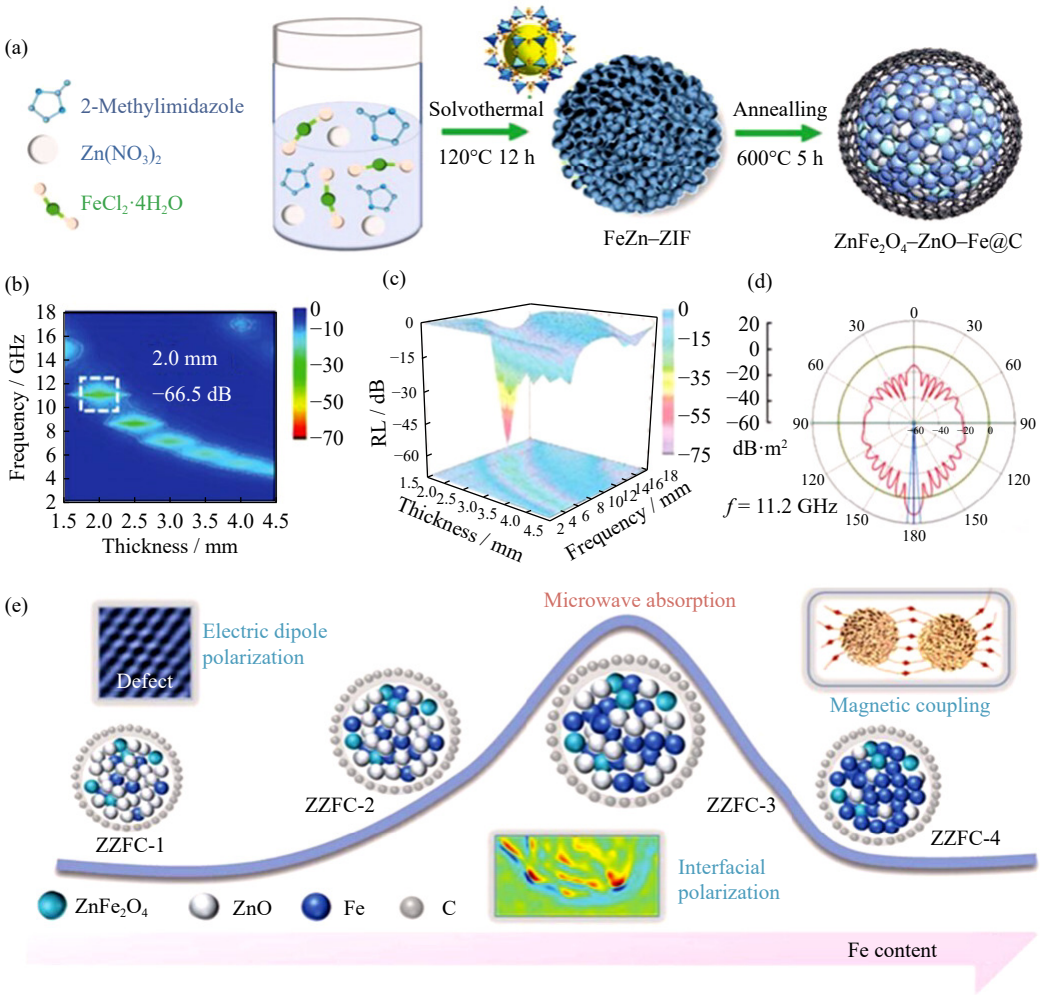

Fig. 13. (a) Synthesis procedure and (b, c) reflection loss curves of ZZFC-3; (d) 2D RCS plots for PEC substrate covered with ZZFC, (e) EMW absorption mechanism of ZZFC. M. Huang, L. Wang, K. Pei, *et al.*, *Adv. Funct. Mater.*, 34, 2308898 (2024) [102]. Copyright Wiley-VCH GmbH. Reproduced with permission.

vantages and disadvantages of ferrite-based EMW absorbers prepared through these four methods. It also provides important guidance and reference for researchers to design high-performance EMW absorption materials based on ferrite.

Acknowledgements

This work was financially supported by the National Natural Science Foundation of China (No.52377026), Taishan Scholars and Young Experts Program of Shandong Province, China (No. tsqn202103057), and the Natural Science Foundation of Shandong Province, China (No. ZR2024ME046).

Conflicts of Interest

Guanglei Wu is an editorial board member for this journal and was not involved in the editorial review or the decision to publish this article. The authors declare no conflict of interest.

References

[1] S.J. Zhang, D. Lan, J.J. Zheng, *et al.*, Perspectives of nitrogen-doped carbons for electromagnetic wave absorption, *Carbon*, 221(2024), art. No. 118925.

[2] X.G. Su, J. Wang, T. Liu, *et al.*, Controllable atomic migration in microstructures and defects for electromagnetic wave absorption enhancement, *Adv. Funct. Mater.*, 34(2024), No. 39, art. No. 2403397.

[3] Z.R. Jia, X.Y. Zhang, Z. Gu, and G.L. Wu, MOF-derived Ni–Co bimetal/porous carbon composites as electromagnetic wave absorber, *Adv. Compos. Hybrid Mater.*, 6(2022), No. 1, art. No. 28.

[4] X.B. Xie, R.L. Liu, C. Chen, *et al.*, Phase changes and electromagnetic wave absorption performance of XZnC (X = Fe/Co/Cu) loaded on melamine sponge hollow carbon composites, *Int. J. Miner. Metall. Mater.*, 32(2025), No. 3, p.566.

[5] J.P. Li, X.P. Liu, H.Y. Zhao, *et al.*, Dual-Phase engineering of Ni_3S_2/NiCo-MOF nanocomposites for enhanced ion storage and electron migration, *Chem. Eng. J.*, 489(2024), art. No. 151069.

[6] D.L. Tan, Q. Wang, M.R. Li, *et al.*, Magnetic media synergistic carbon fiber@Ni/NiO composites for high-efficiency electromagnetic wave absorption, *Chem. Eng. J.*, 492(2024), art. No. 152245.

[7] L.X. Gai, H.H. Zhao, X.A. Li, *et al.*, Shell engineering afforded dielectric polarization prevails and impedance amelioration toward electromagnetic wave absorption enhancement in nested-network carbon architecture, *Chem. Eng. J.*, 501(2024), art. No. 157556.

Table 1. Ferrite-based EMW absorbers fabricated *via* HSPM, SGM, CCPM, and STM

Materials	Synthetic method	Thickness / mm	EAB / GHz	RL_{min} / dB	Mechanism	Ref.
$Ba_{1-x}Ca_xFe_{12}O_{19}$	HSPM	2.0	2.2	−30.8	1	[48]
$FeCo/CoFe_2O_4$/CNFs	HSPM	1.95	5.0	−52.3	2	[49]
$Sr_{0.85}La_{0.15}(MnZr)_xFe_{12-2x}O_{19}$	HSPM	1.1	7.97	−47.8	1	[50]
Hollow $SrFe_{12}O_{19}$	HSPM	3.4	—	−12.69	1	[51]
$ZnFe_2O_4$@PPy	HSPM	3.5	4.1	−41.0	2	[52]
Bulk Ni–Zn ferrite	HSPM	2.1	2.7	−48.1	1	[53]
$Ba(ZrNi)_{0.6}Fe_{10.8}O_{19}$	SGM	2.8	6.24	−17.11	1	[60]
$BaFe_{12-2x}Ni_xTi_xO_{19}$	SGM	0.95	10.05	−52	1	[61]
$Y_{1-x}Sr_xFeO_3$	SGM	2.2	2.4	−30.87	1	[62]
$Ni_{0.5}Zn_{0.5}Fe_2O_4/SrFe_{12}O_{19}$	SGM	4.0	6.4	−47.0	1	[63]
PANI/$NiFe_2O_4$/GN	SGM	2.5	—	−30	2	[64]
$Ti_3C_2T_X$/CNZFO/PANI	CCPM	2.2	4.1	−37.1	2	[73]
MoS_2@NC@$CoFe_2O_4$	CCPM	2.4	3.5	−46.7	2	[74]
RGO/PT@$NiFe_2O_4$	CCPM	2.0	4.6	−45.4	2	[75]
RGO@PANI@TiO_2	CCPM	1.5	—	−45.4	2	[76]
3D-ZFO/GNs	CCPM	1.5	5.56	−31.66	2	[77]
$Cu_2S/CoFe_2O_4$	CCPM	2.1	6.64	−66.58	2	[78]
$ZnFe_2O_4$@PHCMS	STM	4.8	3.52	−51.43	2	[93]
C@$Ni_xCo_{1-x}Fe_2O_4$	STM	1.9	3.3	−51	2	[94]
MXene/NZFO	STM	1.609	4.74	−66.2	2	[95]
$CoFe_2O_4$/CoFe@C	STM	2.17	5.9	−51	2	[97]
Co–$CoFe_2O_4$@PCHMs	STM	2.1	8.48	−65.31	2	[98]
NRGO/$Ni_{0.5}Mg_{0.5}Fe_2O_4$	STM	3.6	—	−56.8	2	[99]
$NiFe_2O_4$/GNs	STM	2.9	—	−57.4	2	[100]
$FeCo/CoFe_2O_4$	STM	1.4	4.7	−51.6	2	[101]
$ZnFe_2O_4$–ZnO–Fe@C	STM	2.0	—	−66.5	2	[102]
$CoFe_2O_4$@PPy-rGO	STM	3.6	13.12	−50.1	2	[34]
$MoS_2/CuFe_2O_4$	STM	2.3	8.16	−40.33	2	[103]
$ZnFe_2O_4$/CC	STM	2.5	4.9	−46.0	2	[104]

Note: 1—Magnetic loss; 2—Synergistic dielectric loss and magnetic loss.

[8] L.M. Song, Y.Q. Chen, Q.C. Gao, *et al.*, Low Weight, low thermal Conductivity, and highly efficient electromagnetic wave absorption of three-dimensional graphene/SiC-nanosheets aerogel, *Compos. Part A: Appl. Sci. Manuf.*, 158(2022), art. No. 106980.

[9] F.Y. Hu, X.H. Wang, S. Bao, *et al.*, Tailoring electromagnetic responses of delaminated $Mo_2TiC_2T_x$ MXene through the decoration of Ni particles of different morphologies, *Chem. Eng. J.*, 440(2022), art. No. 135855.

[10] D.S. Wang, Y.Z. Hu, Z.Y. Cui, *et al.*, Sulfur vacancy regulation and multipolarization of Ni_xCo1S nanowires-decorated biotemplated structures to promote microwave absorption, *J. Colloid Interface Sci.*, 646(2023), p. 991.

[11] D.S. Wang, A. Mukhtar, K.M. Wu, L.Y. Gu, and X.M. Cao, Multi-segmented nanowires: A high tech bright future, *Materials*, 12(2019), No. 23, art. No. 3908.

[12] Z.H. Zhou, X.F. Zhou, D. Lan, *et al.*, Modulation engineering of electromagnetic wave absorption performance of layered double hydroxides derived hollow metal carbides integrating corrosion protection, *Small*, 20(2024), No. 8, art. No. 2305849.

[13] K. Le Anh Cao, A.M. Rahmatika, Y. Kitamoto, M.T.T. Nguyen, and T. Ogi, Controllable synthesis of spherical carbon particles transition from dense to hollow structure derived from Kraft lignin, *J. Colloid Interface Sci.*, 589(2021), p. 252.

[14] Z. Liu, X.L. Fan, M.Y. Han, *et al.*, Branched fluorine/adamantane interfacial compatibilizer for PBO fibers/cyanate ester wave-transparent laminated composites, *Chin. J. Chem.*, 41(2023), No. 8, p. 939.

[15] X.Y. Ren, Y.H. Song, Z.G. Gao, Y.L. Wu, Z.R. Jia, and G.L. Wu, Rational manipulation of composition and construction toward Zn/Co bimetal hybrids for electromagnetic wave absorption, *J. Mater. Sci. Technol.*, 134(2023), p. 254.

[16] C. Srinivas, K. Naga Praveen, E. Ranjith Kumar, *et al.*, Microwave absorption properties of rare earth (RE) ions doped Mn–Ni–Zn nanoferrites (RE = Dy, Sm, Ce, Er) to shield electromagnetic interference (EMI) in X-band frequency, *Ceram. Int.*, 48(2022), No. 22, p. 33891.

[17] D.D. Xiang, Q.C. He, D. Lan, Y.Q. Wang, and X.M. Yin, Regulating the phase composition and microstructure of Fe_3Si/SiC nanofiber composites to enhance electromagnetic wave absorption, *Chem. Eng. J.*, 498(2024), art. No. 155406.

[18] X.L. Chen, T. Shi, G.L. Wu, and Y. Lu, Design of molybdenum disulfide@polypyrrole compsite decorated with Fe_3O_4 and superior electromagnetic wave absorption performance, *J. Colloid Interface Sci.*, 572(2020), p. 227.

[19] X.L. Chen, F. Zhang, D. Lan, *et al.*, State-of-the-art synthesis strategy for nitrogen-doped carbon-based electromagnetic wave absorbers: From the perspective of nitrogen source, *Adv. Compos. Hybrid Mater.*, 6(2023), No. 6, art. No. 220.

[20] S.J. Zhang, Z.G. Gao, Z.B. Sun, *et al.*, Solid solution strategy for bimetallic metal-polyphenolic networks deriving electromagnetic wave absorbers with regulated heterointerfaces, *Ap-*

pl. Surf. Sci., 611(2023), art. No. 155707.
[21] M. Zhang, L.B. Zhao, W.X. Zhao, *et al*., Boosted electromagnetic wave absorption performance from synergistic induced polarization of SiC_{NWs}@MnO_2@PPy heterostructures, *Nano Res.*, 16(2023), No. 2, p. 3558.
[22] G.H. Wang, Y. Zhao, F. Yang, Y. Zhang, M. Zhou, and G.B. Ji, Multifunctional integrated transparent film for efficient electromagnetic protection, *Nano Micro Lett.*, 14(2022), No. 1, art. No. 65.
[23] Y.F. He, Q. Su, D.D. Liu, *et al*., Surface engineering strategy for MXene to tailor electromagnetic wave absorption performance, *Chem. Eng. J.*, 491(2024), art. No. 152041.
[24] L. Wang, X. Li, Q.Q. Li, *et al*., Oriented polarization tuning broadband absorption from flexible hierarchical ZnO arrays vertically supported on carbon cloth, *Small*, 15(2019), No. 18, art. No. 1900900.
[25] S.J. Zhang, J.J. Zheng, D. Lan, *et al*., Hierarchical engineering on built-in electric field of bimetallic zeolitic imidazolate derivatives towards amplified dielectric loss, *Adv. Funct. Mater*., (2024), art. No. 2413884.
[26] L.M. Song, F. Zhang, Y.Q. Chen, *et al*., Multifunctional SiC@SiO_2 nanofiber aerogel with ultrabroadband electromagnetic wave absorption, *Nano Micro Lett.*, 14(2022), No. 1, art. No. 152.
[27] L.M. Song, B.B. Fan, Y.Q. Chen, *et al*., Ultralight and hyperelastic SiC nanofiber aerogel spring for personal thermal energy regulation, *J. Adv. Ceram.*, 11(2022), No. 8, p. 1235.
[28] S.J. Zhang, D. Lan, J.J. Zheng, *et al*., Rational construction of heterointerfaces in biomass sugarcane-derived carbon for superior electromagnetic wave absorption, *Int. J. Miner. Metall. Mater.*, 31(2024), No. 12, p. 2749.
[29] S. Golchinvafa and S.M. Masoudpanah, Magnetic and microwave absorption properties of $FeNi_3$/$NiFe_2O_4$ composites synthesized by solution combustion method, *J. Alloy. Compd.*, 787(2019), p. 390.
[30] L.M. Song, C.W. Wu, Q. Zhi, *et al*., Multifunctional SiC aerogel reinforced with nanofibers and nanowires for high-efficiency electromagnetic wave absorption, *Chem. Eng. J.*, 467(2023), art. No. 143518.
[31] M. Yuan, M. Zhou, and H.Q. Fu, Synergistic microstructure of sandwich-like $NiFe_2O_4$@SiO_2@MXene nanocomposites for enhancement of microwave absorption in the whole Ku-band, *Compos. Part B: Eng.*, 224(2021), art. No. 109178.
[32] X. Yang, L.X. Xuan, W.W. Men, *et al*., Carbonyl iron/glass fiber cloth composites: Achieving multi-spectrum stealth in a wide temperature range, *Chem. Eng. J.*, 491(2024), art. No. 151862.
[33] G.X. Ding, C.X. Chen, H.X. Tai, *et al*., Structural characterization and microwave absorbing performance of $CuFe_2O_4$/RGO composites, *J. Solid State Chem.*, 297(2021), art. No. 122051.
[34] L. Ding, X.X. Zhao, Y. Huang, J. Yan, T.H. Li, and P.B. Liu, Ultra-broadband and covalently linked core–shell $CoFe_2O_4$@PPy nanoparticles with reduced graphene oxide for microwave absorption, *J. Colloid Interface Sci.*, 595(2021), p. 168.
[35] J.M. Tang, K.X. Wang, Y.X. Lu, *et al*., Mesoporous core–shell structure $NiFe_2O_4$@polypyrrole micro-rod with efficient electromagnetic wave absorption in C, X, Ku wavebands, *J. Magn. Magn. Mater.*, 514(2020), art. No. 167268.
[36] X.J. Zhang, G.S. Wang, W.Q. Cao, *et al*., Enhanced microwave absorption property of reduced graphene oxide (RGO)–$MnFe_2O_4$ nanocomposites and polyvinylidene fluoride, *ACS Appl. Mater. Interfaces*, 6(2014), No. 10, p. 7471.
[37] Z.Q. Guo, D. Lan, C.H. Zhang, *et al*., "Two birds one stone" strategy to integrate electromagnetic wave absorption and self-anticorrosion in magnetic nanocomposites with double-shell hollow structure, *J. Mater. Sci. Technol*., 220(2025), p. 307.
[38] Y.M. Lei, Z.J. Yao, H.Y. Lin, A. Ali Haidry, J.T. Zhou, and P.J. Liu, Synthesis and high-performance microwave absorption of reduced graphene oxide/Co-doped ZnNi ferrite/polyaniline composites, *Mater. Lett.*, 236(2019), p. 456.
[39] Y. Zhang, X.H. Liu, Z.Q. Guo, *et al*., MXene@Co hollow spheres structure boosts interfacial polarization for broadband electromagnetic wave absorption, *J. Mater. Sci. Technol.*, 176(2024), p. 167.
[40] S. Chen, Y.B. Meng, X.L. Wang, *et al*., Hollow tubular MnO_2/MXene (Ti_3C_2, Nb_2C, and V_2C) composites as high-efficiency absorbers with synergistic anticorrosion performance, *Carbon*, 218(2024), art. No. 118698.
[41] Y.Y. Lian, D. Lan, X.D. Jiang, *et al*., Multifunctional electromagnetic wave absorbing carbon fiber/$Ti_3C_2T_X$ MXene fabric with superior near-infrared laser dependent photothermal antibacterial behaviors, *J. Colloid Interface Sci.*, 676(2024), p. 217.
[42] Z.X. Liu, Y.Q. Wang, Z.R. Jia, *et al*., *In situ* constructed honeycomb-like $NiFe_2O_4$@Ni@C composites as efficient electromagnetic wave absorber, *J. Colloid Interface Sci.*, 608(2022), p. 2849.
[43] Y.P. Wang, Y.Y. Zhang, J.N. Tao, *et al*., $Co_{0.2}Fe_{2.8}O_4$/C composite nanofibers with designable 3D hierarchical architecture for high-performance electromagnetic wave absorption, *Ceram. Int.*, 47(2021), No. 16, p. 23275.
[44] X.X. Zhao, Y. Huang, J. Yan, *et al*., Excellent electromagnetic wave absorption properties of the ternary composite $ZnFe_2O_4$@PANI–rGO optimized by introducing covalent bonds, *Compos. Sci. Technol.*, 210(2021), art. No. 108801.
[45] D.P. Kozlenko, N.M. Belozerova, S.S. Ata-Allah, *et al*., Neutron diffraction study of the pressure and temperature dependence of the crystal and magnetic structures of $Zn_{0.3}Cu_{0.7}Fe_{1.5}Ga_{0.5}O_4$ polycrystalline ferrite, *J. Magn. Magn. Mater.*, 449(2018), p. 44.
[46] J.Y. Hu, X.S. Liu, X.C. Kan, *et al*., Characterization of texture and magnetic properties of $Ni_{0.5}Zn_{0.5}Ti_xFe_{2-x}O_4$ spinel ferrites, *J. Magn. Magn. Mater.*, 489(2019), art. No. 165411.
[47] Y. Liu, X.Y. Ren, X.F. Zhou, *et al*., Defect design and vacancy engineering of $NiCo_2Se_4$ spinel composite for excellent electromagnetic wave absorption, *Ceram. Int.*, 50(2024), No. 22, p. 46643.
[48] G.L. Feng, W.C. Zhou, C.H. Wang, *et al*., Microwave absorption of M-type hexaferrite $Ba_{1-x}Ca_xFe_{12}O_{19}$ ($x \leq 0.4$) ceramics in 2.6–18 GHz, *Ceram. Int.*, 45(2019), No. 6, p. 7102.
[49] J.B. Chen, J. Zheng, Q.Q. Huang, F. Wang, and G.B. Ji, Enhanced microwave absorbing ability of carbon fibers with embedded FeCo/$CoFe_2O_4$ nanoparticles, *ACS Appl. Mater. Interfaces*, 13(2021), No. 30, p. 36182.
[50] P. Kaur, S. Bahel, and S.B. Narang, Broad-band microwave absorption of $Sr_{0.85}La_{0.15}(MnZr)_xFe_{12-2x}O_{19}$ hexagonal ferrite in 18–40 GHz frequency range, *J. Magn. Magn. Mater.*, 460(2018), p. 489.
[51] Z.H. Wang, L. Zhao, P.H. Wang, L. Guo, and J.H. Yu, Low material density and high microwave-absorption performance of hollow strontium ferrite nanofibers prepared *via* coaxial electrospinning, *J. Alloy. Compd.*, 687(2016), p. 541.
[52] Z.L. Li, H. Zhu, L.J. Rao, *et al*., Wrinkle structure regulating electromagnetic parameters in constructed core–shell $ZnFe_2O_4$@PPy microspheres as absorption materials, *Small*, 20(2024), No. 16, art. No. 2308581.
[53] Y. Zhang, J. Wang, Q.L. Wu, *et al*., Enhanced electromagnetic wave absorption of bacterial cellulose/reduced graphene oxide aerogel by eco-friendly *in situ* construction, *J. Colloid Interface Sci.*, 678(2025), p. 648.
[54] K. Praveena, K. Sadhana, H.L. Liu, N. Maramu, and G. Himanandini, Improved microwave absorption properties of TiO_2 and $Ni_{0.53}Cu_{0.12}Zn_{0.35}Fe_2O_4$ nanocomposites potential for mi-

crowave devices, *J. Alloy. Compd.*, 681(2016), p. 499.
[55] X.G. Su, Y. Zhang, J. Wang, and Y.Q. Liu, Enhanced electromagnetic wave absorption and mechanical performances of graphite nanosheet/PVDF foams *via* ice dissolution and normal pressure drying, *J. Mater. Chem. C*, 12(2024), No. 21, p. 7775.
[56] Z.Q. Guo, D. Lan, Z.R. Jia, *et al*., Multiple tin compounds modified carbon fibers to construct heterogeneous interfaces for corrosion prevention and electromagnetic wave absorption, *Nano Micro Lett.*, 17(2024), No. 1, art. No. 23.
[57] X.L. Chen, X.W. Wang, L.D. Li, and S.H. Qi, Preparation and microwave absorbing properties of nickel-coated carbon fiber with polyaniline via *in situ* polymerization, *J. Mater. Sci. Mater. Electron.*, 27(2016), No. 6, p. 5607.
[58] M. Banerjee, A. Mukherjee, S. Chakrabarty, S. Basu, and M. Pal, Bismuth-doped nickel ferrite nanoparticles for room temperature memory devices, *ACS Appl. Nano Mater.*, 2(2019), No. 12, p. 7795.
[59] Y.N. Yang, L. Xia, T. Zhang, *et al*., Fe_3O_4@LAS/RGO composites with a multiple transmission-absorption mechanism and enhanced electromagnetic wave absorption performance, *Chem. Eng. J.*, 352(2018), p. 510.
[60] Y.T. Zhang, C.Y. Liu, K.S. Peng, Y.F. Cao, G. Fang, and Y.J. Zhang, Synthesis of broad microwave absorption bandwidth Zr^{4+}–Ni^{2+} ions gradient-substituted barium ferrite, *Ceram. Int.*, 46(2020), No. 16, p. 25808.
[61] S.J. Cheon, J.R. Choi, S.B. Lee, J.I. Lee, and H. Lee, Frequency tunable Ni–Ti-substituted Ba–M hexaferrite for efficient electromagnetic wave absorption in 8.2–75 GHz range, *J. Alloy. Compd.*, 976(2024), art. No. 173019.
[62] M. Wang, L.C. Cheng, L. Huang, *et al*., Effect of Sr doped the $YFeO_3$ rare earth ortho-ferrite on structure, magnetic properties, and microwave absorption performance, *Ceram. Int.*, 47(2021), No. 24, p. 34159.
[63] Q.X. Han, X.F. Meng, and C.H. Lu, Exchange-coupled $Ni_{0.5}Zn_{0.5}Fe_2O_4/SrFe_{12}O_{19}$ composites with enhanced microwave absorption performance, *J. Alloy. Compd.*, 768(2018), p. 742.
[64] X.L. Chen and S.H. Qi, Preparation and microwave absorbing properties of polyaniline/$NiFe_2O_4$/graphite nanosheet composites via sol–gel reaction and *in situ* polymerization, *J. Sol Gel Sci. Technol.*, 81(2017), No. 3, p. 824.
[65] S.J. Zhang, Y.X. Pei, Z.W. Zhao, C.L. Guan, and G.L. Wu, Simultaneous manipulation of polarization relaxation and conductivity toward self-repairing reduced graphene oxide based ternary hybrids for efficient electromagnetic wave absorption, *J. Colloid Interface Sci.*, 630(2023), p. 453.
[66] M. Ben Ali, K. El Maalam, H. El Moussaoui, *et al*., Effect of zinc concentration on the structural and magnetic properties of mixed Co–Zn ferrites nanoparticles synthesized by sol/gel method, *J. Magn. Magn. Mater.*, 398(2016), p. 20.
[67] N.N. Ali, R. Al-Qassar Bani Al-Marjeh, Y. Atassi, A. Salloum, A. Malki, and M. Jafarian, Design of lightweight broadband microwave absorbers in the X-band based on (polyaniline/Mn-NiZn ferrite) nanocomposites, *J. Magn. Magn. Mater.*, 453(2018), p. 53.
[68] H. Li, Z.M. Cao, J.Y. Lin, *et al*., Synthesis of u-channelled spherical $Fe_x(Co_yNi_{1-y})_{100-x}$ Janus colloidal particles with excellent electromagnetic wave absorption performance, *Nanoscale*, 10(2018), No. 4, p. 1930.
[69] C. Aoopngan, J. Nonkumwong, S. Phumying, *et al*., Amine-functionalized and hydroxyl-functionalized magnesium ferrite nanoparticles for Congo red adsorption, *ACS Appl. Nano Mater.*, 2(2019), No. 8, p. 5329.
[70] P. Iranmanesh, S.T. Yazdi, M. Mehran, and S. Saeednia, Superior magnetic properties of Ni ferrite nanoparticles synthesized by capping agent-free one-step coprecipitation route at different pH values, *J. Magn. Magn. Mater.*, 449(2018), No., p. 172.
[71] T.B. Zhao, D. Lan, Z.R. Jia, Z.G. Gao, and G.L. Wu, Hierarchical porous molybdenum carbide synergic morphological engineering towards broad multi-band tunable microwave absorption, *Nano Res.*, 17(2024), No. 11, p. 9845.
[72] F.A. Wahaab, L.L. Adebayo, A.A. Adekoya, I.G. Hakeem, B. Alqasem, and A.M. Obalalu, Physiochemical properties and electromagnetic wave absorption performance of $Ni_{0.5}Cu_{0.5}Fe_2O_4$ nanoparticles at X-band frequency, *J. Alloy. Compd.*, 836(2020), art. No. 155272.
[73] Y.M. Lei, Z.J. Yao, S.Z. Li, J.T. Zhou, A. Ali Haidry, and P.J. Liu, Broadband high-performance electromagnetic wave absorption of Co-doped NiZn ferrite/polyaniline on MXenes, *Ceram. Int.*, 46(2020), No. 8, p. 10006.
[74] X.L. Chen, W. Wang, T. Shi, G.L. Wu, and Y. Lu, One pot green synthesis and EM wave absorption performance of MoS_2@nitrogen doped carbon hybrid decorated with ultrasmall cobalt ferrite nanoparticles, *Carbon*, 163(2020), p. 202.
[75] P.B. Liu, Y. Huang, and X. Zhang, Superparamagnetic $NiFe_2O_4$ particles on poly(3,4-ethylenedioxythiophene)–graphene: Synthesis, characterization and their excellent microwave absorption properties, *Compos. Sci. Technol.*, 95(2014), p. 107.
[76] P.B. Liu, Y. Huang, J. Yan, and Y. Zhao, Magnetic graphene@PANI@porous TiO_2 ternary composites for high-performance electromagnetic wave absorption, *J. Mater. Chem. C*, 4(2016), No. 26, p. 6362.
[77] J.T. Zhou, B. Wei, M.Q. Wang, *et al*., Three dimensional flower like $ZnFe_2O_4$ ferrite loaded graphene: Enhancing microwave absorption performance by constructing microcircuits, *J. Alloy. Compd.*, 889(2021), art. No. 161734.
[78] T.T. Zheng, Y. Zhang, Z.R. Jia, J.H. Zhu, G.L. Wu, and P.F. Yin, Customized dielectric-magnetic balance enhanced electromagnetic wave absorption performance in $Cu_xS/CoFe_2O_4$ composites, *Chem. Eng. J.*, 457(2023), art. No. 140876.
[79] F. Zhang, W. Cui, B.B. Wang, *et al*., Morphology-control synthesis of polyaniline decorative porous carbon with remarkable electromagnetic wave absorption capabilities, *Compos. Part B: Eng.*, 204(2021), art. No. 108491.
[80] T.Q. Hou, Z.R. Jia, A.L. Feng, *et al*., Hierarchical composite of biomass derived magnetic carbon framework and phytic acid doped polyanilne with prominent electromagnetic wave absorption capacity, *J. Mater. Sci. Technol.*, 68(2021), p. 61.
[81] T.T. Cheng, Y.Y. Guo, Y.X. Xie, *et al*., Customizing the structure and chemical composition of ultralight carbon foams for superior microwave absorption performance, *Carbon*, 206(2023), p. 181.
[82] H.Q. Li, Y.H. Hou, and L.C. Li, Tunable design of yolk–shell $ZnFe_2O_4$@C composites for enhancing electromagnetic wave absorption, *Powder Technol.*, 378(2021), p. 216.
[83] L.G. Ren, Y.Q. Wang, Z.R. Jia, Q.C. He, and G.L. Wu, Controlling the heterogeneous interfaces of Fe_3O_4/N-doped porous carbon *via* facile swelling for enhancing the electromagnetic wave absorption, *Compos. Commun.*, 29(2022), art. No. 101052.
[84] C.H. Sun, D. Lan, Z.R. Jia, Z.G. Gao, and G.L. Wu, Kirkendall effect-induced ternary heterointerfaces engineering for high polarization loss MOF–LDH–MXene absorbers, *Small*, 20(2024), No. 48, art. No. 2405874.
[85] S. Golchinvafa, S.M. Masoudpanah, and M. Jazirehpour, Magnetic and microwave absorption properties of FeCo/$CoFe_2O_4$ composite powders, *J. Alloy. Compd.*, 809(2019), art. No. 151746.
[86] N. Matinise, X.G. Fuku, K. Kaviyarasu, N. Mayedwa, and M. Maaza, ZnO nanoparticles via Moringa oleifera green synthes-

is: Physical properties & mechanism of formation, *Appl. Surf. Sci.*, 406(2017), p. 339.

[87] Z.R. Jia, L.F. Sun, Z.G. Gao, and D. Lan, Modulating magnetic interface layer on porous carbon heterostructures for efficient microwave absorption, *Nano Res.*, 17(2024), No. 11, p. 10099.

[88] D.W. Chu, F.B. Li, X.M. Song, *et al*., A novel dual-tasking hollow cube $NiFe_2O_4$–NiCo–LDH@rGO hierarchical material for high preformance supercapacitor and glucose sensor, *J. Colloid Interface Sci.*, 568(2020), p. 130.

[89] Y. Yuan, S.C. Wei, Y. Liang, *et al*., Solvothermal assisted synthesis of $CoFe_2O_4$/CNTs nanocomposite and their enhanced microwave absorbing properties, *J. Alloy. Compd.*, 867(2021), art. No. 159040.

[90] T. Ma, Y. Cui, Y.L. Sha, *et al*., Facile synthesis of hierarchically porous rGO/MnZn ferrite composites for enhanced microwave absorption performance, *Synth. Met.*, 265(2020), art. No. 116407.

[91] R.V. Lakshmi, P. Bera, R.P.S. Chakradhar, *et al*., Enhanced microwave absorption properties of PMMA modified $MnFe_2O_4$–polyaniline nanocomposites, *Phys. Chem. Chem. Phys.*, 21(2019), No. 9, p. 5068.

[92] T.T. Zheng, Z.R. Jia, Q.Q. Zhan, *et al*., Self-assembled multilayered hexagonal-like MWCNTs/MnF_2/CoO nanocomposite with enhanced electromagnetic wave absorption, *Carbon*, 186(2022), p. 262.

[93] L. Chai, Y.Q. Wang, N.F. Zhou, *et al.*, *In-situ* growth of core-shell $ZnFe_2O_4$ @ porous hollow carbon microspheres as an efficient microwave absorber, *J. Colloid Interface Sci.*, 581(2021), p. 475.

[94] X.L. Chen, Y. Wang, H.L. Liu, S. Jin, and G.L. Wu, Interconnected magnetic carbon@$Ni_xCo_{1-x}Fe_2O_4$ nanospheres with core–shell structure: An efficient and thin electromagnetic wave absorber, *J. Colloid Interface Sci.*, 606(2022), p. 526.

[95] S.Y. Guo, H.L. Guan, Y. Li, *et al*., Dual-loss $Ti_3C_2T_x$ MXene/$Ni_{0.6}Zn_{0.4}Fe_2O_4$ heterogeneous nanocomposites for highly efficient electromagnetic wave absorption, *J. Alloy. Compd.*, 887(2021), art. No. 161298.

[96] P.F. Yin, L.M. Zhang, P. Sun, *et al*., Apium-derived biochar loaded with $MnFe_2O_4$@C for excellent low frequency electromagnetic wave absorption, *Ceram. Int.*, 46(2020), No. 9, p. 13641.

[97] J.W. Ge, S.M. Liu, L. Liu, *et al*., Optimizing the electromagnetic wave absorption performance of designed hollow $CoFe_2O_4$/CoFe@C microspheres, *J. Mater. Sci. Technol.*, 81(2021), p. 190.

[98] H.X. Zhang, Z.R. Jia, B.B. Wang, *et al*., Construction of remarkable electromagnetic wave absorber from heterogeneous structure of Co–$CoFe_2O_4$@mesoporous hollow carbon spheres, *Chem. Eng. J.*, 421(2021), art. No. 129960.

[99] R.W. Shu, L.L. Xu, and Z.W. Zhao, Construction of a hollow nickel–magnesium ferrite decorated nitrogen-doped reduced graphene oxide composite aerogel for highly efficient and broadband microwave absorption, *J. Mater. Chem. C*, 11(2023), No. 48, p. 16961.

[100] Y.Y. Ma, Y.H. Jiang, C.Y. Wang, S.B. Kang, G.Q. Chen, and B. Zhong, Microwave absorption performance enhancement of $NiFe_2O_4$/GNs composite with hollow hexagonal-like structure, *J. Magn. Magn. Mater.*, 565(2023), art. No. 170281.

[101] M. Liu, B. Zhao, K. Pei, *et al*., An ion-engineering strategy to design hollow FeCo/$CoFe_2O_4$ microspheres for high-performance microwave absorption, *Small*, 19(2023), No. 25, art. No. 2300363.

[102] M.Q. Huang, L. Wang, K. Pei, *et al*., Heterogeneous interface engineering of bi-metal MOFs-derived $ZnFe_2O_4$–ZnO-Fe@C microspheres via confined growth strategy toward superior electromagnetic wave absorption, *Adv. Funct. Mater.*, 34(2024), No. 3, art. No. 2308898.

[103] J.K. Liu, Z.R. Jia, W.H. Zhou, *et al*., Self-assembled MoS_2/magnetic ferrite $CuFe_2O_4$ nanocomposite for high-efficiency microwave absorption, *Chem. Eng. J.*, 429(2022), art. No. 132253.

[104] X.L. Chen, D. Lan, L.T. Zhou, *et al*., Rational construction of $ZnFe_2O_4$ decorated hollow carbon cloth towards effective electromagnetic wave absorption, *Ceram. Int.*, 50(2024), No. 13, p. 24549.